

HELSINKI INSTITUTE OF PHYSICS

INTERNAL REPORT SERIES

HIP-2018-01

# Electroweak phase transition in theories beyond the Standard Model

Tuomas V. I. Tenkanen

Helsinki Institute of Physics  
University of Helsinki  
Finland

ACADEMIC DISSERTATION

*To be presented, with the permission of the Faculty of Science of the University of Helsinki, for public criticism in the auditorium A111 at Exactum, Gustaf Hällströmin katu 2 B, Helsinki, on the 3rd of May 2018 at 10.00 o'clock.*

Helsinki 2018

ISBN 978-951-51-1273-6 (print)

ISBN 978-951-51-1274-3 (pdf)

ISSN 1455-0563

<http://ethesis.helsinki.fi>

Unigrafia

Helsinki 2018



---

T. V. I. Tenkanen: Electroweak phase transition in theories beyond the Standard Model,  
University of Helsinki, 2018, 45 pages,  
Helsinki Institute of Physics, Internal Report Series, HIP-2018-01,  
ISBN 978-951-51-1273-6,  
ISSN 1455-0563.

## Abstract

Non-perturbative analysis provides the most accurate information about the properties of the electroweak phase transition in the Standard Model of particle physics. In this thesis, we initiate similar non-perturbative studies for three theories of physics beyond the Standard Model. Properties of the phase transition are important for both obtaining reliable predictions for potential gravitational wave background produced by this phase transition, and for viability of electroweak baryogenesis, that attempts to solve the problem of observed matter/antimatter asymmetry of the universe.

In particular, we study three models with an extended Higgs sector: the Two-Higgs-Doublet Model, the real singlet and the real triplet extensions of the Standard Model. In all these models we have derived three-dimensional effective theories by using a method of high temperature dimensional reduction. The main result of this thesis is a set of dimensional reduction matching relations between parameters of effective theories and physical quantities in the aforementioned extensions of the Standard Model. In certain regions of parameter space for each model, we are able to perform a non-perturbative analysis simply by recycling lattice results obtained in the past. For a full analysis, new simulations are required, which goes beyond the scope of this thesis.

In this thesis, we provide a brief introduction to the electroweak phase transition and electroweak baryogenesis. We then discuss both perturbative and non-perturbative approaches to the problem in greater detail. Finally, we summarise and discuss the results obtained so far, and outline future directions for research.

## Acknowledgements

I thank my supervisors Aleksi Vuorinen and David J. Weir for their guidance, support and encouragement. In particular, I thank AV for trusting me to take a lot of responsibility in our projects, and DJW for teaching me many valuable things in physics and life.

I wish to express my gratitude to all my other collaborators as well. In particular, I thank Tomáš Brauner for teaching me quantum field theory; Tyler Gorda, Andreas Helset and Jonathan Kozachuk for discussions and Anders Tranberg and Jens Andersen for their hospitality in UiS and NBIA. I thank Hiren Patel and Michael J. Ramsey-Musolf for inspiration and collaboration. I am especially grateful for MJRM for inviting me to visit UMass and for his role in creating an inspiring atmosphere in ACFI. I have huge respect for the irreplaceable contributions made by Lauri Niemi to our research projects. I sincerely thank LN for all his efforts and for me, our collaboration has been a great privilege.

I am thankful for enlightening discussions with Keijo Kajantie, Mikko Laine and Kari Rumukainen. I thank pre-examiners Aleksi Kurkela and Sami Nurmi for reading and commenting this thesis. The research presented in this thesis has been funded mostly by Vilho, Yrjö and Kalle Väisälä Foundation and I acknowledge their financial support.

My current and former fellow graduate students and neighbours from A313 – Arttu, Tommi, Vera-Maria, Jere, Jarkko, Sara, Joni, Eemeli and Eemeli – deserve cheerful fist bumps. In addition I thank my other co-students and now friends Petri, Sebastian, Panu, Kalle, Juho, Karoliina, Johann, Marko, Johanna and Eveliina: it has been great to know you and hang out together during my almost eight years in Helsinki. I thank Lasse and Risto, and all the experimentalists, for sharing an office for many years. I happily cherish the memories of many late nights spent in Beckwith Park with Kimmo and Mika. In addition, I thank Tommi Mäkelä for co-operation in the very early stages of my doctoral studies. Especially, I want to thank my close friend Jarkko for many memorable occasions and Tommi for sharing a dream and ambition to understand and admire the universe we live in.

Finally, I thank my family for being part of my life – I wish to give special shout-outs to Joonas, Jesse, Juuso and Hilma – and also thanks to Sara’s family: I am deeply grateful for all the time I have spent in Turku and Velkua with you. I’m most grateful of all to Sara for facing many ups and downs of life with me and sharing a home in Viikki together with Nytyi and Oona.

---

## List of included papers

This thesis is based on the following publications [1–4]:

### **I Dimensional reduction of the Standard Model coupled to a new singlet scalar field**

T. Brauner, T. V. I. Tenkanen, A. Tranberg, A. Vuorinen and D. J. Weir  
JHEP **1703**, 007 (2017) [arXiv:1609.06230v2]

### **II On the nature of the electroweak phase transition in the two Higgs doublet model**

J. O. Andersen, T. Gorda, A. Helset, L. Niemi, T. V. I. Tenkanen, A. Tranberg, A. Vuorinen and D. J. Weir  
[arXiv:1711.09849v3]

### **III Electroweak phase transition and dimensional reduction of the Two-Higgs Doublet Model**

T. Gorda, A. Helset, L. Niemi, T. V. I. Tenkanen and D. J. Weir  
[arXiv:1802.05056v1]

### **IV Electroweak phase transition in the $\Sigma$ SM - I: Dimensional reduction**

L. Niemi, H. H. Patel, M. J. Ramsey-Musolf, T. V. I. Tenkanen and D. J. Weir  
[arXiv:1802.10500]

In all of the papers the authors are listed alphabetically according to particle physics convention.

## The author's contribution

In all of the papers, in collaboration, the author performed all the computations involved – except tree-level relations to physical parameters in II and III, or phenomenological constraints in IV – and participated in all numerical analysis and in writing of all articles.

# Contents

Abstract . . . . .	iv
Acknowledgements . . . . .	v
List of Included Papers . . . . .	vi
<b>1 Introduction</b>	<b>1</b>
1.1 Electroweak phase transition . . . . .	2
1.2 Electroweak baryogenesis . . . . .	4
<b>2 Thermodynamics of the transition</b>	<b>8</b>
2.1 Perturbation theory and effective potential . . . . .	9
2.2 Non-perturbative methods . . . . .	13
2.2.1 Dimensional reduction and three-dimensional effective theories . . . . .	13
2.2.2 $SU(2) \times U(1)$ + Higgs doublet effective theory . . . . .	15
2.2.3 Determination of physical quantities . . . . .	19
<b>3 Character and strength of EWPT in BSM theories</b>	<b>22</b>
3.1 Standard Model . . . . .	23
3.2 Two-Higgs-Doublet Model . . . . .	25
3.3 Singlet extended Standard Model . . . . .	30
3.4 Standard Model with a real triplet . . . . .	32
<b>4 Review and outlook</b>	<b>35</b>
<b>Bibliography</b>	<b>39</b>

# Chapter 1

## Introduction

The discovery of the Higgs boson at the LHC has filled a major missing piece of the Standard Model (SM) of particle physics [5, 6]. While colliders continue their search for any evidence of further physics beyond the Standard Model (BSM), a direct detection of gravitational waves (GW) from black hole and neutron star binary mergers was achieved by LIGO and Virgo [7, 8]. Future gravitational wave detector projects, such as the space-based detector LISA [9], can probe physics in the connection between elementary particle physics and cosmology, by searching for evidence of cosmological phase transitions [10, 11]. One such transition is the electroweak phase transition (EWPT), where electroweak symmetry is spontaneously broken by the Higgs field in the early, cooling universe [12, 13]. While the EWPT in the SM would have been a mild cross-over [14–17] – which does not produce a detectable stochastic GW signature – extensions of the SM could provide strong first-order phase transitions, that may be detectable.

Many BSM theories have been proposed to solve open issues in particle physics and cosmology. In modern cosmology the explanation for the observed matter/antimatter asymmetry in the present universe remains as one of the major unsolved problems [18]. One of the candidates for explanation is the mechanism of electroweak baryogenesis (EWBG) [19], where observed asymmetry is generated during the EWPT. For the EWBG to be viable, the EWPT has to be a strong first-order transition. This requires a new BSM field whose mass is not far from the electroweak scale and that couples directly to the Higgs, in order to make the transition – that is driven by the Higgs field – stronger. This implies that new physics could be discovered in upcoming collider and precision experiments, should EWBG to be realised in nature. This testability of EWBG makes it an attractive candidate to solve the problem of matter/antimatter asymmetry.

In the research presented in this thesis, in Papers I-IV, our aim is to eventually quantify thermodynamic properties of the EWPT, and to deliver accurate predictions for the cosmic GW background and the EWBG in several BSM theories. Concretely, we present results for the character, strength and critical temperature of the EWPT for three well-motivated extensions of the Standard Model. In the remainder of this chapter, we present a qualitative introduction to the EWPT and the EWBG. In Chapter 2 we present a more detailed discussion of the EWPT,

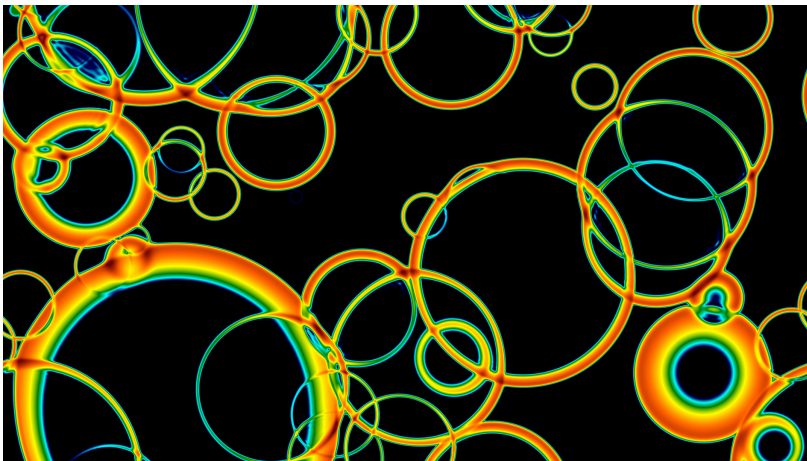


Figure 1.1: A classical field-fluid simulation of bubbles from a first order cosmological phase transition. Figure by D. J. Weir, see Ref. [20].

and in particular discuss different methods that can be used to analyse it. In Chapter 3 we briefly introduce three BSM theories that have been studied in Papers I-IV – real-singlet and real-triplet extensions of the SM and the Two-Higgs Doublet Model – and present preliminary results for thermodynamic properties of the EWPT in these models. Finally, in Chapter 4 we summarise and discuss future prospects of our studies.

## 1.1 Electroweak phase transition

The initial conditions assumed for the EWPT are a hot, radiation-dominated early universe containing zero net baryon number. See [21, 22] for reviews of EWBG that discuss the EWPT, and relevant discussion about the EWPT in Refs. [23, 24]. In the transition the thermal plasma goes from a symmetric state – in which the full electroweak gauge invariance is manifest – to a broken state where only the electromagnetic subgroup remains. The transition from symmetric to broken phase can be characterized by the vacuum expectation values of the scalar fields that are involved in the transition.

For a detectable GW signature as well as for viable baryogenesis, a necessary – but not sufficient – condition is that transition is of first order. This means that at some critical value for the temperature, there is a discontinuity in the order parameter of the theory. If there is a potential barrier between the two phases, a first-order transition occurs through thermal or quantum nucleation of bubbles of the broken phase [25, 26]. A wall forms, separating the bubbles of the broken phase from the surrounding symmetric phase, and bubbles expand, collide and merge together eventually filling the whole universe, see Fig. 1.1. Collisions of the bubbles induce shear stresses that source gravitational waves [27, 28]. In addition, large scale simulations

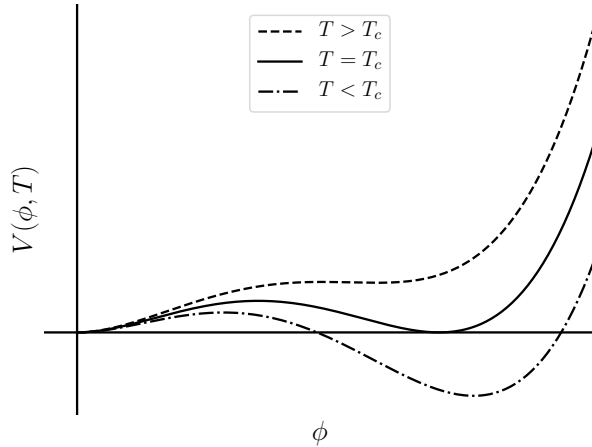


Figure 1.2: Shape of the effective potential near the critical temperature. In first-order transition, there is a barrier between minima at  $T_c$ , and as  $T$  decreases there is a discontinuous jump in the Higgs expectation value.

have shown that even after the bubbles have merged together and disappeared, sound waves in the surrounding plasma remain and continue producing gravitational waves [29]. Furthermore, these bubbles are critical for the EWBG as well. In the SM, the EWPT is a cross-over [30] – which means that there is no discontinuous change in any derivative of order parameter – and there is no bubble nucleation during the transition.

Frequently, the EWPT is studied perturbatively in terms of the finite-temperature effective potential (see Section 2.1 for a formal definition), which corresponds to the free-energy of the cosmic plasma that is close to thermodynamic equilibrium. The value of this potential is minimised by the expectation value of the Higgs field. At temperatures above the critical temperature  $T_c$ , the global minimum of the potential is at the origin. At  $T_c$ , there is another minimum – at a non-zero value of the field – that is degenerate with the minimum at the origin, and at lower temperatures, this other minimum becomes deeper, as illustrated in Fig. 1.2. In a first-order transition, there is a barrier between the minima at  $T_c$  and the bubbles will nucleate at a temperature slightly below this.

The most relevant equilibrium features of the EWPT are its strength and character – whether the transition is of first or second order, or a cross-over – the critical temperature, and latent heat and interface tension between symmetric and broken phases. Important non-equilibrium properties include the bubble nucleation temperature, the bubble nucleation rate and speed and profile of the bubble walls. For the EWBG also crucial is the sphaleron transition rate, that

describes the rate of baryon number generation and washout, as we discuss later in this chapter.

These features have been studied frequently using perturbative methods, in different BSM theories, see for e.g. [31–39]. However, it is known that the application of perturbation theory to the EWPT contains many theoretical uncertainties – and furthermore – even ambiguities, mostly due to problems associated with infrared physics [40, 41], as well as gauge invariance [42, 43]. A more robust computation of many of the above quantities can be performed using non-perturbative Monte Carlo methods [14, 16, 44]. In Chapter 2, we discuss these issues in detail.

Finally, we emphasize that gravitational waves from first order phase transition [10, 20, 45] can open a new window into the physics of the early universe and underlying theories of particle physics. In a first-order transition at the electroweak scale, gravitational waves are produced at frequencies that coincide with the peak sensitivity of LISA. One of the science goals of LISA is detecting a stochastic GW signal of cosmological origin, but on the other hand, if LISA does not see evidence for a cosmological phase transition, BSM theories could be constrained. Furthermore, phase transitions in the dark matter sector of the universe could also be studied in addition to the EWPT [46].

Relatively few parameters are required to describe the GW power spectrum of the EWPT – the phase transition strength, inverse transition duration, bubble wall velocity and critical temperature. Despite this, the resulting physics is complicated, and requires large simulations. For quantitatively reliable studies of the EWPT in different BSM theories, it is crucial to obtain accurate predictions for these quantities.

## 1.2 Electroweak baryogenesis

Explaining the origin of the observed matter/antimatter asymmetry of the universe remains as an outstanding problem at the interface of particle physics and cosmology. This asymmetry can be characterized by the baryon to entropy density ratio

$$Y_B \equiv \frac{\rho_B}{s} = (8.61 \pm 0.09) \times 10^{-11}, \quad (1.1)$$

or, alternatively, by comparing the baryon density  $\rho_B$  to the photon density  $\rho_\gamma$ . The baryon density is simply the number of baryons per unit volume, and the entropy density  $s$  is given by the sum of pressure and density (given by the energy-momentum tensor) over temperature. At the current Cosmic Microwave Background (CMB) temperature of 2.725 K, the photon density  $\rho_\gamma \approx 411$  photons/cm<sup>3</sup> and the entropy density  $s \approx 7.04\rho_\gamma$ .

The ratio  $Y_B$  can be measured either from the light element (particularly deuterium) abundance generated by Big Bang Nucleosynthesis [47], or from the baryon acoustic oscillations of the CMB, where the relative magnitudes of Doppler peaks in the temperature anisotropy are sensitive to the asymmetry [48]. Practically, it is not reasonable to assume that this baryon asymmetry was present as an initial condition of the universe, as it would have been washed out

by the cosmic inflation. For this reason, this asymmetry needs to be generated dynamically in the process referred to as baryogenesis.

In our discussion, we will focus on the electroweak baryogenesis (EWBG), where the generation of the baryon asymmetry happens during the EWPT. See for reviews [21–23, 49]. However, we emphasize that several other mechanisms for baryogenesis have been suggested. One such attempt is the leptogenesis, where baryon asymmetry is generated dynamically from the lepton asymmetry [50]. In leptogenesis the SM is extended with right-handed Majorana neutrinos with very large mass parameters of order  $10^{15}$  GeV. These mass terms explicitly violate lepton number conservation, and when the temperature of the universe drops below this mass scale, heavy neutrinos decay into lighter particles through lepton violating interactions. This generates a lepton asymmetry, which can then be turned into a baryon asymmetry by sphaleron transitions (see discussion below). Additional motivation for the leptogenesis scenario is that these large Majorana mass terms for right-handed neutrinos explain naturally the tiny masses of left-handed SM neutrinos, through the see-saw mechanism, as the physical mass eigenvalues for light neutrinos are suppressed by the heavy mass scale.

Other mechanisms for baryogenesis include the Affleck-Dine mechanism [51] similar to leptogenesis, or the Peskin-Anderson mechanism [52] – mechanisms that both utilise inflationary dynamics. See also Ref. [53]. All these scenarios, other than EWBG, involve very large mass scales compared to the electroweak scale, and their biggest shortcoming is that they are not testable with the current – nor near-future – range of particle collider energies. This is not necessarily true for EWBG, and this is what makes this scenario attractive.

Any early universe particle physics mechanism that attempts to explain the baryon asymmetry, has to satisfy three general criteria – known as the Sakharov conditions [54]:

- Violation of baryon number
- Violation of C and CP
- Departure from thermal equilibrium

First condition follows immediately from assumption that the universe starts with zero baryon number (defined as difference of baryons and antibaryons), and currently non-zero baryon number is observed. Second condition stands for violations of symmetries of both charge conjugation (C) and combined charge conjugation and parity (CP). These conditions are required for the rate of total baryon production to be different to total anti-baryon production. Finally, a departure from thermal equilibrium is required. This is related to the CPT symmetry, that is, the combined symmetry of CP and time reversal (T). The CPT symmetry is a property of any unitary, Lorentz invariant quantum field theory. The baryon number changes sign under C transformation, but is invariant under P and T transformations. From these properties, it follows that a thermal average of baryon number at equilibrium vanishes. However, if universe has departed from thermal equilibrium at some stage, this conclusion is not valid. For example, in leptogenesis, departure from thermal equilibrium occurs when the temperature decreases below

the mass scale of heavy neutrinos and they decay into Higgs bosons and left-handed leptons. An alternative way of ensuring that universe deviates from thermal equilibrium, is a first-order phase transition.

For the EWBG, in principle all these required conditions could have been realised in the pure SM. Due to the CKM-matrix – where at least one CP-violating phase must remain in Higgs-quark interactions despite field redefinitions – the weak interactions involve C and CP violation. The weak interactions in the SM also violate baryon number conservation due to a chiral anomaly. Indeed, a classical chiral symmetry is violated at one-loop by triangle diagrams contributing to rate of pion decay  $\pi^0 \rightarrow \gamma\gamma$  [55, 56]. The SU(2) gauge bosons of weak interactions couple only to left-handed fermions, and consequently the chiral anomaly leads to currents that produce non-conservation of baryon and lepton numbers (yet B-L is conserved).

Field configurations of these anomalous currents have non-trivial topological structure, and in analogy to topological solitons, they can be associated with quasi-particles with localised energy density. One such field configuration – or a quasi-particle – is the sphaleron [57, 58], which is particularly relevant for baryogenesis [59, 60]. The sphaleron is a static, unstable solution to the classical equations of motion, that geometrically represents a saddle point of the electroweak potential. Sphaleron process cannot be described by perturbative methods. Another quasi-particle is the electroweak instanton, which is the minimum energy solution in four Euclidean dimensions. The instanton process, physically corresponding to a tunneling through two minima with different baryon numbers, converts three baryons into three antileptons, or three antibaryons into three leptons. In a similar manner, the sphaleron violates baryon and lepton numbers but it corresponds physically to classically crossing over the barrier between two minima. Both the instanton and sphaleron processes are heavily suppressed at zero-temperature. However, the key feature of the sphaleron is that sphaleron rate is unsuppressed if the electroweak symmetry is restored. This means, that in the symmetric phase in the early universe before EWPT, the baryon non-conserving processes are rapid compared to the expansion of the universe.

Finally, in EWBG – that occurs during the EWPT – a departure from thermal equilibrium is provided by a first-order transition via bubble nucleation. In EWBG, baryon creation takes place in the vicinity of the expanding bubble walls. When the underlying theory contains CP violation, scattering of particles in the plasma from bubble walls can generate CP asymmetries of particles and antiparticles in front of the bubble wall. In the symmetric phase – in front of the bubble wall – rapid electroweak sphaleron transitions produce a net excess of baryons over antibaryons. The expanding bubble wall devours some of the net excess of baryons, and inside the bubble in the broken phase, sphaleron transitions are rapidly turned off – provided that the transition is strong enough. This ensures that the net creation of baryons does not get washed out. Therefore a first-order transition is not a sufficient condition for the EWBG; one has to make sure that transition is strong enough.

However, in the minimal SM, despite the fact that sphaleron processes are present, the other conditions immediately rule out EWBG: in the SM the EWPT is a cross-over, and further-

more, CP-violating effects within the SM are severely suppressed at high temperatures [61–65]. Therefore, for EWBG, physics beyond the SM is essential.

In the research presented in this thesis, we limit our interest to identifying parameter space regions where a first-order transition occurs, and computing the strength and critical temperature of the EWPT in three different BSM theories, that provide necessary, but not sufficient conditions for EWBG. In order to make conclusions about the viability of EWBG in a given BSM theory, it is important to produce robust theoretical predictions for the thermodynamic properties of the EWPT together with the phenomenological implications for collider physics. Furthermore, a strong first-order phase transition capable of emitting significant amounts of gravitational waves would provide a signal that could be detected by LISA. We emphasize, however, that for stronger gravitational wave production, large bubble wall velocities are preferable, whereas for EWBG the relative wall velocity compared to the velocity of the plasma in front of the bubble wall has to be smaller than the speed of sound [66]. In this sense, there is some tension between these two different motivations to study the EWPT.

## Chapter 2

# Thermodynamics of the transition

At the moment, the most accurate predictions can be made for equilibrium thermodynamic properties of the transition, such as the existence and order of the transition, the critical temperature  $T_c$ , the latent heat and the surface tension. Knowledge about the equilibrium thermodynamics provides a necessary starting point for evaluation of non-equilibrium processes, such as sphaleron and bubble nucleation rates, which are crucial for validity of EWBG and possible gravitational wave signatures of the EWPT.

The thermodynamic properties of the system are described by the partition function and its derivatives. For a pedagogical review, see [24, 67]. By using the Euclidean imaginary time formalism – that connects statistical mechanics to quantum field theory – the path integral representation of the partition function can be constructed as

$$Z(T) = \int \mathcal{D}\Phi e^{-S[\Phi]} \quad (2.1)$$

where  $\Phi$  includes all the fields in the theory and  $S$  is an action in Euclidean space. In the Euclidean action, the temporal dimension (imaginary time) is restricted to compact interval from 0 to  $1/T$ , where  $T$  is the temperature of the system. For bosons, periodic boundary conditions are imposed, and antiperiodic for fermions. As a consequence of these boundary conditions, the fields can be written in Matsubara decomposition as an infinite sum of spatial 3-d fields

$$\Phi(x, \tau) = \sqrt{T} \sum_{-\infty}^{\infty} \varphi_n(x) e^{i\omega_n \tau}, \quad (2.2)$$

where  $\tau$  is imaginary time and the phase factor is given by the Matsubara frequency  $\omega_n$ , equal to  $2n\pi T$  for bosons and  $(2n+1)\pi T$  for fermions. Using this decomposition, one can perform the integral over imaginary time in the action, and as a result the action can be written as integral over spatial dimensions and sum over the Matsubara frequencies. The theory at finite temperature can therefore be shown to correspond to a 3-d Euclidean theory with an infinite number of fields.

In different BSM theories, these properties of the EWPT have frequently been studied by using perturbative methods and, in particular, the finite-temperature effective potential [31–39].

We begin this chapter by introducing this perturbative approach and its downsides, motivating why it is important to examine the validity and accuracy of this method. We then introduce an alternative, non-perturbative approach in terms of three dimensional effective theories. Effective theories are obtained by dimensional reduction, where all non-zero Matsubara modes are integrated out. The latter approach provides a theoretically more robust framework for analysis of the EWPT, and in all Papers I-IV this approach is utilised.

## 2.1 Perturbation theory and effective potential

A generating functional is defined by including a source functional  $J$  in the path integral (where  $\Phi$  is now a single scalar field, for simplicity)

$$e^{W[J]} \equiv \int \mathcal{D}\Phi e^{-S[\Phi]-J\Phi}. \quad (2.3)$$

The functional  $W[J]$  is the generator of all connected diagrams in perturbation theory. The effective action is defined as a Legendre transformation of  $W[J]$

$$\Gamma[\phi] \equiv W[J] - \int J(x)\phi(x) d^4x, \quad (2.4)$$

where the order parameter function  $\phi \equiv \delta W[J]/\delta J$  is a classical field. Finally, the effective potential  $V(\phi)$  – which is a function of the classical field – is defined by

$$\Gamma[\phi] \equiv - \int V(\phi) d^4x. \quad (2.5)$$

By using the property that the effective action can be written as expansion of 1-particle irreducible (1PI) Green's functions  $\Gamma^{(n)}$ , with some manipulation one can show that the effective potential can be expressed as

$$V(\phi) = - \sum_{n=0}^{\infty} \frac{1}{n!} \phi^n \Gamma_0^{(n)}. \quad (2.6)$$

Here the subscript zero denotes that the 1PI Green's functions are evaluated at vanishing external momenta. Close to thermodynamic equilibrium, the effective potential coincides with the free energy of the cosmological plasma and quantities like the order, the critical temperature, and the latent heat of the phase transition can be determined from it. In gauge field theories, the procedure outlined above contains subtleties, related to gauge fixing in the path integral.

For determination of the effective potential, there exists a simple recipe: shift the quantum fields  $\Phi$  in the Lagrangian by a classical background field  $\phi$ , and calculate all 1PI vacuum diagrams in the shifted theory, to desired loop order. At one-loop level, the effective potential is of the form [22]

$$V_{\text{eff}}(\phi, T) = V_0(\phi) + V_1(\phi) + \Delta V_T(\phi, T) + \Delta V_{\text{daisy}}(\phi, T), \quad (2.7)$$

where  $V_0$  is a tree-level potential. The one-loop correction at zero-temperature reads

$$V_1(\phi) = \sum_i \frac{(-1)^{2s_i} n_i}{4(4\pi)^2} \left(m_i^2(\phi)\right)^2 \left( \ln \left( \frac{m_i^2(\phi)}{\Lambda^2} \right) + C_i \right), \quad (2.8)$$

where  $i$  sums over all the fields of  $n_i$  degrees of freedom and spin  $s_i$ . The squared mass eigenvalues  $m_i^2$  depend on the background field  $\phi$ .  $\Lambda$  is the renormalisation scale in dimensional regularisation, with scheme-dependent constants  $C_i$ . Choosing an RG-scale equal to the largest mass squared eigenvalue eliminates the largest logarithm, and optimises the perturbation expansion. The finite temperature parts are given by

$$\Delta V_T(\phi, T) = \sum_i \frac{n_i}{2\pi^2} T^4 J_b \left( \frac{m_i^2}{T^2} \right) - \sum_j \frac{n_j}{2\pi^2} T^4 J_f \left( \frac{m_j^2}{T^2} \right), \quad (2.9)$$

where  $i, j$  run over bosons and fermions, respectively, and  $J_b$  and  $J_f$  are bosonic and fermionic thermal functions, that are related to the free energies of the relativistic boson – or fermion – gas. Finally, the daisy- or ring-resummation contribution reads

$$\Delta V_{\text{daisy}}(\phi, T) = \frac{T^2}{12\pi} \sum_i \left( \left( m^2(\phi) + \Pi(T) \right)_i^{\frac{3}{2}} - m_i^2(\phi)^{\frac{3}{2}} \right), \quad (2.10)$$

where the sum runs over scalars and the longitudinal components of the gauge fields, and  $\Pi(T)$  are the corresponding one-loop thermal masses. This daisy-resummation term is related to the infrared (IR) behaviour of the theory, and we shall now discuss this in greater detail.

### Infrared behaviour

The IR-behaviour can be analysed by considering the daisy diagram illustrated in Fig. 2.1, where the momentum of the large loop  $P = (0, \vec{p})$  has vanishing Matsubara frequency, while  $N$  smaller loops have momenta  $Q$  with non-zero Matsubara frequencies. This diagram is proportional to (each vertex giving coupling squared  $g^2$ )

$$\propto g^{2N} T \int_p \frac{1}{(p^2 + m^2)^N} \left( \sum_Q \frac{1}{Q^2} \right)^N \propto m^3 T \left( \frac{gT}{m} \right)^{2N}, \quad (2.11)$$

where we have omitted an overall combinatorial factor. Definitions and results for these integrals can be found in Appendix C of Paper III. For a gauge field in the broken phase  $m = \frac{1}{2}g\phi$ , and therefore this contribution is of order  $O(g^3)$  for any  $N$ , and furthermore, IR-divergent for  $N > 1$  in the limit  $\phi \rightarrow 0$ . This IR-problem can be partially cured by a daisy resummation [24]: one must first calculate the thermal corrections from the non-zero modes to get corrected mass of the zero-mode, and only then integrate a loop over the zero-mode with the thermal corrected mass. For gauge fields this thermal mass is referred as the Debye mass, and it physically arises as a screening mass due to the heat bath.

This procedure can be applied to scalar fields and the temporal components of gauge fields. For instance, the  $A_0^a$  field (the temporal component of SU(2) gauge field with isospin  $a$ ) obtains a

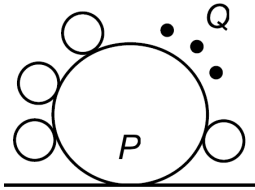


Figure 2.1: Daisy diagram with an IR-sensitive contribution, when momentum of the large loop  $P = (0, \vec{p})$  has vanishing Matsubara frequency, while  $N$  smaller loops have momenta  $Q$  with non-zero Matsubara frequencies. Figure originally from Ref. [67].

resummed mass squared  $\frac{1}{4}g^2\phi^2 + cg^2T^2$ , and in the limit  $\phi \rightarrow 0$  this is non-zero and therefore IR-finite (the factor  $c$  is a numerical constant). Unfortunately, one cannot generate perturbatively a correction to spatial components of gauge fields  $A_i^a$ , and the IR-problems related to zero-modes of these remain.

Due to these IR-problems at finite temperature, the perturbative expansion parameters of a finite temperature system differ from those of the same system at zero temperature [40, 41]. Despite the system being weakly coupled at zero temperature, at high temperatures the expansion parameter might not be small, making the calculation unreliable. In particular, the symmetric phase always remains non-perturbative.

### Physical quantities

In the case of the SM, the leading behaviour of the effective potential at high temperature can be written as

$$V_{\text{eff}}(\phi, T) = \left( DT^2 - \frac{1}{2}\mu^2 \right) \phi^2 - ET\phi^3 + \frac{\lambda}{4}\phi^4 + \dots \quad (2.12)$$

where  $\mu^2$  and  $\lambda$  are the tree-level squared mass parameter and quartic coupling, respectively, and  $D$  and  $E$  are temperature independent functions of couplings of the theory. The critical temperature  $T_c$  and the location of the broken minimum  $\phi_c$  can be solved from the conditions

$$V(\phi_c, T_c) = 0, \quad (2.13)$$

$$\frac{\partial V(\phi_c, T_c)}{\partial \phi} = 0, \quad (2.14)$$

i.e. the symmetry-breaking minimum becomes degenerate with the minimum at the origin. When the coefficient of the cubic term  $E$  is nonzero, there is a first order phase transition at temperature  $T_c$  and the minima are separated by a barrier. The strength of the transition is conventionally characterised by the ratio of location of the broken minimum and the critical temperature, that is

$$\frac{\phi_c}{T_c} = \frac{2E}{\lambda}, \quad (2.15)$$

to leading order. However, note that this quantity is gauge dependent, and therefore not a physical quantity. Thermodynamic quantities, such as the latent heat ( $L$ ) and the surface tension ( $\sigma$ ) between the symmetric and broken phases, characterise the strength of transition. The surface tension can be obtained from the effective potential as

$$\sigma = \int_0^{\phi_c(T_c)} \sqrt{2V(\phi)} d\phi. \quad (2.16)$$

The latent heat is the difference of the energy densities in the symmetric and broken phase at  $T_c$ , and since the effective potential is related to the energy density  $\rho$  by  $V = \rho - Ts$ , where the entropy density  $s \equiv -\partial V/\partial T$ , we have the relation

$$L = T_c \left( \frac{\partial V(\phi_c, T_c)}{\partial T} - \frac{\partial V(0, T_c)}{\partial T} \right). \quad (2.17)$$

Both the surface tension and the latent heat increase as the transition becomes stronger.

### Disadvantages of the perturbative approach

In the previous section we described how to find the critical temperature from the condition of degenerate minima. This requires knowledge of the value of the effective potential in the broken and symmetric minima. However, while the former quantity can be determined – since perturbation theory is applicable at sufficiently large  $\phi$  – the latter quantity cannot be known accurately in perturbation theory, due to infrared problems related to the symmetric phase. Note that due to arbitrariness in overall normalisation, the absolute value of the potential does not have any physical meaning.

This means that an accurate determination of the critical temperature of the phase transition is beyond the scope of perturbation theory [44, 68]. This is also true for the bubble nucleation temperature, since the computation of the bubble nucleation rate requires the knowledge of the effective action for small  $\phi$ . Therefore, determination of these quantities in perturbation theory always involves theoretical uncertainty. For this reason, a reliable determination of these quantities requires non-perturbative methods, in practise lattice Monte Carlo simulations [14, 16]. In non-perturbative studies of the SM, considerable deviations from perturbative computations of the effective potential were found at small  $\phi$ . Therefore, in studies of the EWPT in BSM theories, use of non-perturbative studies is essential.

Finally, we highlight that the perturbative approach utilising the effective potential suffers also from issues of gauge-dependency. In Eq. (2.15) the coefficient  $E$  is heavily gauge dependent, and that gauge-dependency remains in higher order contributions, and therefore  $\phi_c/T_c$  is not a physical quantity that describes the strength of transition. Indeed, while the value of the extrema of the potential are gauge-invariant, the location of these extrema are gauge-dependent. In Refs. [42, 43] this issue of gauge dependency is discussed in the context of perturbation theory.

## 2.2 Non-perturbative methods

In principle the most direct way to perform a non-perturbative study is to regulate the full four dimensional euclidean theory on a lattice. In lattice regularisation, the path integral in Eq. (2.1) is discretised on a finite lattice with lattice spacing  $a$  and total number of lattice sites  $V$ . The path integral is then performed numerically by Monte Carlo (MC) integration methods, for fixed  $a$  and  $V$ . In these MC simulations, the physical result is then obtained by extrapolation, where one takes  $a \rightarrow 0$  and  $V \rightarrow \infty$ , the continuum and thermodynamic limits, respectively.

However, it turns out that that in order to study the EWPT, it is not necessary to perform simulations of the full four-dimensional theory. Instead, one can derive an effective three-dimensional theory which is purely spatial, assuming that the temperature is high compared to other mass scales. This 3-d approach is based on a method called high temperature dimensional reduction [69–71].

### 2.2.1 Dimensional reduction and three-dimensional effective theories

In the imaginary time formalism of the finite- $T$  quantum field theory, at high temperatures, the masses of the non-zero Matsubara modes are of order  $\pi T$ . This scale is referred to as *superheavy*, and non-zero modes decouple from the three-dimensional zero-modes that have masses of order  $gT$  – a scale referred to as *heavy* – where  $g$  is the perturbative coupling. Consequently, the non-zero modes can be integrated out in the first step of dimensional reduction, and dynamics of the system can be described by an effective three dimensional theory at the heavy scale that contains only the zero modes. These include the original scalar and gauge fields, as well as temporal scalar fields, that are remnants of the temporal components of the 4-d gauge fields. Furthermore, near the critical temperature, the mass parameter of the 3-d field driving the transition becomes small due to the cancellation of tree-level value and loop corrections, and parametrically the mass can be described as being of order  $g^2 T$  – a scale dubbed *light*. This allows one to further simplify the effective theory by integrating out the heavy scale, in order to study the properties of the transition at the light scale in the vicinity of the critical temperature. Therefore, in the second step of the dimensional reduction, the heavy temporal scalars – for which their Debye masses are heavy – are integrated out, in addition to any heavy BSM fields. In the final effective theory at the light scale, the light scalars and gauge fields remain. Scale hierarchy of the high temperature system and the different steps of dimensional reduction are illustrated in Fig. 2.2. For a more detailed discussion of framework of dimensional reduction, see Section 1.2 of Paper I or Refs. [70, 71].

Formally, the parameters of the effective 3-d theory are defined such that the 3-d theory produces the same static Green’s functions for light bosonic degrees of freedom as the original 4-d theory, up to a certain perturbative accuracy. In practice this is obtained by a matching procedure for the correlators in both theories, which is performed perturbatively in the  $\overline{\text{MS}}$  scheme. For the 4-point correlators and Debye masses, one-loop accuracy is sufficient, while

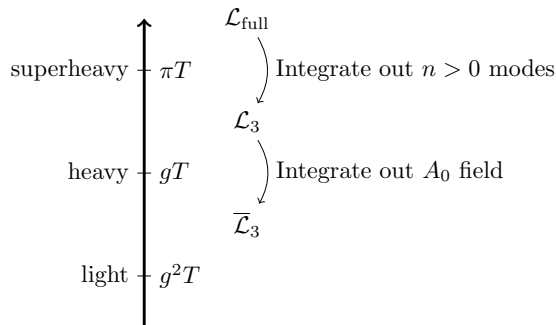


Figure 2.2: Scale hierarchy of the system at high temperature, and construction of effective theories at different steps of the dimensional reduction. In first step, all superheavy non-zero modes are integrated out. In the second step, temporal scalars with heavy Debye masses are integrated out, together with heavy BSM fields. At light scale, light scalars and gauge fields remain.

scalar self-energies are evaluated at two-loop level.

Because the dimensional reduction procedure is perturbative, it is crucial to estimate both its validity and accuracy numerically. Systematic errors are produced from higher order corrections to the effective parameters, and higher order operators that are neglected from the effective theory.

Once the dimensional reduction is performed and the effective theory at the light scale is obtained, one can analyse the properties of the system in the vicinity of critical temperature non-perturbatively, using aforementioned MC simulations. However, in the case of three-dimensional effective theory, simulations are more efficient than in four dimensions. If the errors for the dimensional reduction remain small, and the numerical 3-d MC simulations can match that accuracy, a reliable description of the equilibrium thermodynamics of the system can be provided.

What makes the dimensional reduction a particularly attractive method is a division of the full problem into two parts: perturbative dimensional reduction and MC simulations. Former is free of IR problems and can be performed perturbatively with an acceptable degree of accuracy, and the latter is used to study the dynamics of the light bosonic modes, correctly describing the non-perturbative IR sector. Thus the effective 3-d theory approach implements the required resummations at finite temperature. In addition, there are other reasons why the 3-d approach is a very economical strategy. Unlike in the 4-d simulations, the connection to physical quantities is straightforward, as the zero-temperature renormalisation is made in the perturbative dimensional reduction step. The three-dimensional effective theory is purely bosonic, so there is no need for dynamical fermions on the lattice. In addition, when dimension-6 and higher or-

der operators are neglected in the effective theory, the 3-d theory is superrenormalisable, which allows simple continuum extrapolation from the lattice results. In 3-d simulations the shortest length scale of the high temperature system has been removed by dimensional reduction, which means larger lattice spacing can be used, leading to smaller numerical expense. This is because in lattice simulations the volume of the lattice should be so large that it can accommodate the longest wavelengths, while the lattice spacing should be smaller than the shortest physical length scale in the system.

Finally, the three dimensional effective theory of  $SU(2) \times U(1)$  + Higgs doublet – which we refer as *the SM-like effective 3-d theory* – has a universal character, in the sense that it can describe many different 4-d theories. This means that IR problems and non-perturbative properties for all these 4-d theories can be determined by performing the numerical simulations once. Only thing that changes between different 4-d theories is the DR mapping between 3-d couplings and physical parameters of the underlying theory, and past 3-d simulation results of Refs. [14, 16] can be recycled in the study of EWPT in the BSM theories [72, 73]. As the main result of this thesis, in Papers I,II,III and IV we present dimensional reduction matching relations for three different BSM theories. In addition, many details of the derivations and approximations used are described therein. Because of the universality of the SM-like effective theory, in all these BSM theories we can – at least in limited regions of parameter space for each model – immediately obtain non-perturbative results for the EWPT, with only the DR-mappings at hand. However, we highlight that for comprehensive results for full parameter space of each model, new simulations will be required.

### 2.2.2 $SU(2) \times U(1)$ + Higgs doublet effective theory

The SM-like effective 3-d theory is defined by the Lagrangian

$$\mathcal{L}_{3-d} = \frac{1}{4} G_{ij}^a G_{ij}^a + \frac{1}{4} F_{ij} F_{ij} + (D_i \Phi)^\dagger (D_i \Phi) + m_3^2 \Phi^\dagger \Phi + \lambda_3 (\Phi^\dagger \Phi)^2, \quad (2.18)$$

with  $SU(2)$  and  $U(1)$  gauge couplings  $g_3$  and  $g'_3$ , respectively, and purely spatial indices  $i, j = 1, 2, 3$  and isospin indices  $a = 1, 2, 3$ . In practise, the parameters of the effective theory are complicated functions of the temperature and physical quantities of the full 4-d theory, but since there are many theories that can be mapped onto this effective theory, it is useful to analyse the 3-d theory generally, without a specific choice for the underlying 4-d theory. In this section, we follow Refs. [14, 16].

#### Continuum theory

In three dimensions, in the perturbative treatment in the  $\overline{MS}$  scheme, the only divergences occur for the scalar two-point function at the two-loop level and only the mass parameter requires renormalisation, while the other couplings are RG-invariant. Due to the super-renormalisable nature of the 3-d theory, the two-loop running gives an exact scale dependence for mass parameter. All couplings ( $g_3^2, g_3'^2, m_3^2, \lambda_3$ ) are dimensionful, and therefore one can use any of them

to fix the scale. As in Refs. [14, 16], we fix the scale to  $g_3^2$ . This allows us to directly recycle the results of these references. The dynamics of the system depend only on three dimensionless parameters

$$y \equiv \frac{m_3^2(g_3^2)}{g_3^4}, \quad x \equiv \frac{\lambda_3}{g_3^2}, \quad z \equiv \frac{g_3'^2}{g_3^2}. \quad (2.19)$$

The properties of the phase transition, however, depend essentially only on one parameter, since in practise  $z$  is constant, and  $y$  vanishes near the transition, at leading order. The single parameter that remains is  $x$ , which determines the properties of the transition. It turns out that at small  $x$ , the transition is of first order and gets weaker as  $x$  increases. At  $x \sim 0.11$  there is the end-point of the transition line, and for higher  $x$  the transition is a cross-over. While the first mentioned property is predicted by perturbation theory, the latter is not, but is unique to the non-perturbative analysis.

The dimensionless quantities that we want to determine in the 3-d theory are the critical curve  $y_c(x_c)$  of the phase diagram, the jump  $\Delta l_3 \equiv l_3^b - l_3^s$  of the order parameter  $l_3 \equiv \langle \phi^\dagger \phi(g_3^2) \rangle / g_3^2$  between the broken and symmetric phases at the transition point and the surface tension between two phases. In Section 2.2.3 we describe how these quantities can be related to the critical temperature, latent heat and the surface tension of the phase transition in the 4-d theory. Let us first discuss how these quantities can be obtained in 3-d perturbation theory, and after that discussion, nonperturbatively in 3-d lattice simulations.

A comprehensive perturbative treatment for the SM-like 3-d theory was developed in [68], and applied in [14, 16]. The effective potential is derived at the two-loop level, which is required in order to fix the RG-scale of the theory, and optimise the analysis by doing RG-improvement of the effective potential. This perturbative calculation is performed with dimensional regularisation in the  $\overline{\text{MS}}$ -scheme, in Landau gauge.

The critical curve  $y_c(x_c)$  is given by the condition that the broken minimum is degenerate with the symmetric minimum at the origin, i.e. when  $V(\phi_c) = 0$  and  $dV/d\phi = 0$  at  $\phi = \phi_c$  (we assume that the symmetric minimum is normalised to zero). In perturbation theory, the jump of the order parameter is approximately  $\Delta l_3 \sim \frac{1}{2} \phi_c^2(y_c) / g_3^2$  and

$$\sigma_3 \equiv \int_0^{\phi_c/g_3} \sqrt{\frac{2V(\varphi)}{g_3^6}} d\varphi, \quad (2.20)$$

where  $\varphi \equiv \phi/g_3$  and  $V$  is the effective potential. Results for these quantities in perturbation theory as a function of 3-d parameter  $x$  are given in Figs. 2.4 and 2.5, together with non-perturbative results.

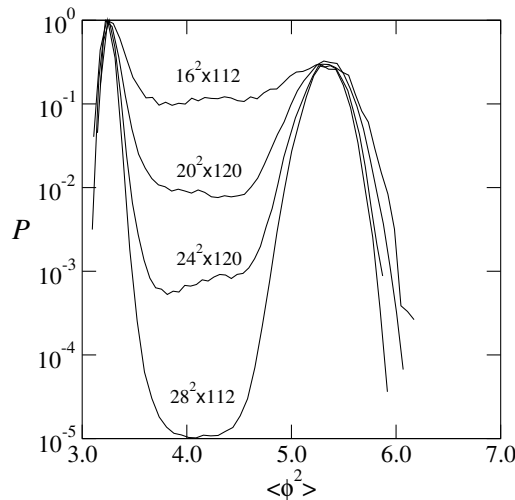


Figure 2.3: Probability distribution of scalar field expectation value at fixed  $x = 0.06444$ ,  $\beta_G = 8$  and various volumes. The double-peak structure reveals a first-order transition. Surface tension can be obtained from the plateau between the peaks, and the latent heat from the distance between the peaks. Figure by K. Rummukainen.

### Lattice regularisation

To obtain non-perturbative results, one has to turn to the lattice. In the lattice regularisation, the 3-d theory of Eq. (2.18) is given by the action

$$\begin{aligned}
 S = & \beta_G \sum_x \sum_{i < j} \left( 1 - \frac{1}{2} \text{Tr} P_{ij} \right) - \beta_H \sum_x \sum_i \frac{1}{2} \text{Tr} \Phi^\dagger(\vec{x}) U_i(\vec{x}) \Phi(\vec{x} + \vec{i}) \\
 & + \sum_x \frac{1}{2} \text{Tr} \Phi^\dagger(\vec{x}) \Phi(\vec{x}) + \beta_R \sum_x \left( \frac{1}{2} \text{Tr} \Phi^\dagger(\vec{x}) \Phi(\vec{x}) - 1 \right)^2, \quad (2.21)
 \end{aligned}$$

where  $\vec{i}$  is a unit vector and where standard link variable reads (to leading order in  $a$ )

$$U_i(\vec{x}) = e^{igaA_i(\vec{x} + \frac{1}{2}\vec{i})}, \quad (2.22)$$

where the gauge field acts as a connection in the parallel transporter between two neighbouring lattice sites. The plaquette – a discretised version of the gauge kinetic term – is built out of links over a closed loop

$$\text{Tr} P_{ij} \equiv \text{Tr} U_i(\vec{x}) U_j(\vec{x} + \vec{i}) U_i^\dagger(\vec{x} + \vec{j}) U_j^\dagger(\vec{x}). \quad (2.23)$$

The dimensionless parameters  $\beta_G, \beta_H$  and  $\beta_R$  are related to the continuum parameters in the

continuum limit  $a \rightarrow 0$  by

$$g_3^2 a = \frac{4}{\beta_G}, \quad (2.24)$$

$$x = \frac{1}{4} \lambda_3 a \beta_G = \frac{\beta_R \beta_G}{\beta_H^2}, \quad (2.25)$$

$$y = \frac{\beta_G^2}{8} \left( \frac{1}{\beta_H} - 3 - \frac{2x\beta_H}{\beta_G} \right) + \frac{3\Sigma\beta_G}{32\pi} (1 + 4x) \\ + \frac{1}{16\pi^2} \left( \left( \frac{51}{16} + 9x - 12x^2 \right) \left( \ln \frac{3\beta_G}{2} + \zeta \right) + 5.0 + 5.2x \right), \quad (2.26)$$

where the constants 5.0, 5.2 and  $\Sigma = 3.17591$ ,  $\zeta = 0.09$  arise from lattice perturbation theory. Because of the super-renormalisability of the 3-d theory, the lattice counterterms evaluated at two-loop order are the exact result. Continuum results are obtained from the lattice simulation results by first extrapolating the lattice measurements to the thermodynamic limit  $V \rightarrow \infty$ , with fixed lattice spacing  $a$  (in practise, fixed  $\beta_G$ ) and then each of the  $V \rightarrow \infty$  values are in turn extrapolated to the continuum limit  $a \rightarrow 0$  ( $\beta_G \rightarrow \infty$ ). The MC simulations are based on measuring gauge invariant composite operator expectation values and distributions, such as average Higgs field squared

$$R^2 = \frac{1}{V} \sum_x \text{Tr} \Phi^\dagger(\vec{x}) \Phi(\vec{x}), \quad (2.27)$$

where sum runs over all lattice sites and  $V$  is the total number of the lattice sites. These simulations are performed using Monte Carlo techniques, that utilise variety of update algorithms. We do not discuss these in this thesis, but refer to Refs. [14]

The existence of the first-order phase transition can be observed from the distribution of the above order parameter, as at the critical values of the 3-d parameters  $x, y, z$ , the distribution of the order parameter develops a double-peak structure, see Fig. 2.3. The latent heat is related to the double-peak structure seen in a first order transition. The expectation value

$$l_3 \equiv \frac{\langle \phi^\dagger \phi(g_3^2) \rangle}{g_3^2}, \quad (2.28)$$

and the difference  $\Delta l_3 \equiv l_3^b - l_3^s$ , at the critical point can be measured as difference of the heights of the two peaks (for technical details, see Ref. [14]) The surface tension is related to how the height of the plateau between the two peaks scales with the cross-sectional area of the lattice. We define a dimensionless quantity

$$\sigma_3 \equiv \lim_{V \rightarrow \infty} \frac{1}{g_3^4 A} \ln \frac{P_{\max}}{P_{\min}}, \quad (2.29)$$

where  $P_{\max}$  and  $P_{\min}$  are the probability distribution maximum and the minimum between the peaks and  $A$  is the smallest cross-sectional area on a three-dimensional periodic volume.

Above we described how these quantities are determined in perturbation theory, and the comparison to the non-perturbative results is given in Figs. 2.4 and 2.5. In perturbation theory the curves continue to large values of  $x$ , but on the lattice – if  $x$  is larger than  $\sim 0.11$  – the first

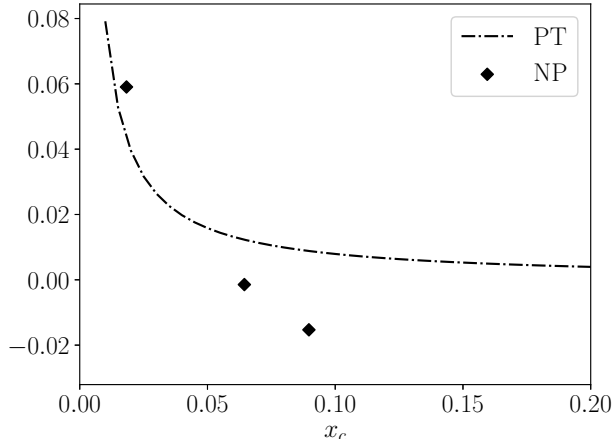


Figure 2.4: The critical  $y_c$  as function of  $x_c$ . Discrete points are nonperturbative (NP) result from Table 10 in Ref. [14], and solid curve is result obtained in the perturbation theory (PT) [16]. The key property of the non-perturbative study is that the first-order transition terminates at  $x \sim 0.11$ . This property is not captured by perturbation theory.

order transition ends and transition becomes a cross-over. When  $x > 0.11$ , on the lattice  $\Delta l_3$  and  $\sigma_3$  vanish. This comparison shows that for small values of  $x$ , the perturbative treatment is a good approximation, yet it crucially fails to describe the endpoint of the critical line at  $x \sim 0.11$ . When  $x$  is very small, the transition becomes strong as indicated by increasing latent heat and surface tension. Strong first order transitions are relevant for gravitational wave production and baryogenesis, and the use of 3-d perturbation theory seems justified. However, a non-perturbative information about the end point of transition provides valuable information as well: for BSM physics to be able to modify the EWPT to be strongly first order, relatively large couplings are required. Thus, the location of the end-point gives the lower limit for the BSM couplings, that can provide a viable setting for gravitational wave production in the EWPT or EWBG.

### 2.2.3 Determination of physical quantities

By using the dimensional reduction matching relations, the 3-d parameters can be related to the temperature and physical quantities of the underlying 4-d theory. Then, the relations between the 3-d observables of the previous section and the 4-d thermodynamics can be derived as in Ref. [14]. Below, we list the results. The critical temperature is obtained from the critical line

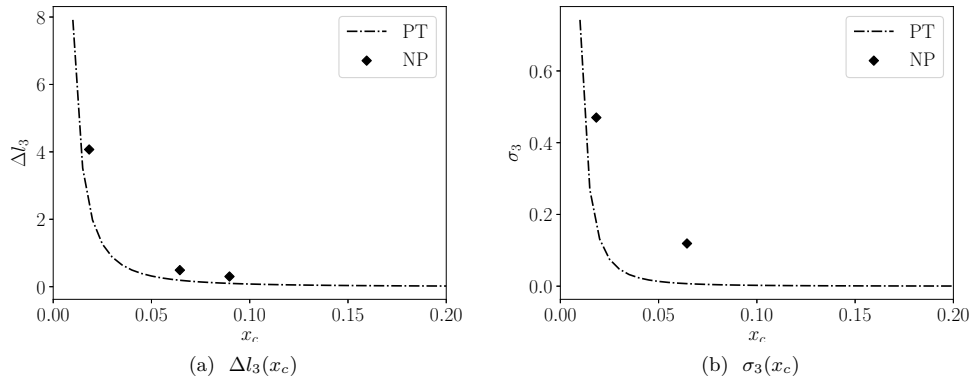


Figure 2.5: As Fig. 2.4, but presenting  $\Delta l_3(x_c)$  and  $\sigma_3(x_c)$ , respectively. These 3-d quantities can be used to derive the latent heat and the surface tension of the the transition.

$y_c(x_c)$ . The surface tension  $\sigma$  can be obtained from

$$\frac{\sigma}{T_c^3} = \sigma_3 \frac{g_3^4}{T_c^2}, \quad (2.30)$$

and the latent heat  $L$  from

$$\frac{L}{T_c^4} = \Delta l_3 \frac{g_3^6}{T_c^2} \left( \frac{dy}{dT} - \frac{dx}{dT} \frac{dy_c}{dx_c} \right). \quad (2.31)$$

Finally, the ratio  $v^2(T_c)/T_c^2 \equiv 2\langle\phi^\dagger\phi(T_c)\rangle/T_c$  can be obtained from

$$\frac{v^2(T_c)}{T_c^2} = 2 \frac{g_3^2}{T_c} \left( l b^3 - \frac{3}{16\pi^2} \ln \frac{g_3^2}{T_c} \right). \quad (2.32)$$

Note that the last quantity is gauge independent, unlike its perturbative counterpart. In all these expressions, the 3-d gauge coupling  $g_3$  is calculated at the critical temperature. By using these relations, one can obtain the above quantities characterising the thermodynamics of the phase transition in any BSM theory that can be mapped into the SM-like effective 3-d theory via dimensional reduction. Generalising these analyses to effective theories with extended scalar sectors, remains as an important future prospect.

In a first order phase transition, colliding bubbles of broken phase produce gravitational waves (together with sound waves in the surrounding plasma). To determine the corresponding power spectra, knowledge of critical and bubble nucleation temperatures, strength and inverse duration of the transition are required. The critical temperature can be obtained as explained above, and transition strength can be related to the latent heat. The bubble nucleation temperature  $T_n$  can be estimated – for instance, in the thin wall approximation – with the use of the latent heat and the surface tension found on the lattice. However, a comprehensive, non-perturbative

determination of  $T_n$  and bubble nucleation rate – to which inverse duration of the transition is related – is more involved than the simple thin wall approximation, yet crucially important, as the errors can be large. Finally, for electroweak baryogenesis, the quantity of interest is the sphaleron transition rate, which in the classical approximation is proportional to the exponential suppression  $\exp(-E_{\text{sph}}/T)$ . This suppression has to be large enough so that an excess of baryons generated outside of the expanding bubble in the symmetric phase, do not get washed out in the broken phase inside the bubble. Here the sphaleron energy  $E_{\text{sph}}$  can be related to the 3-d parameter  $x$  that characterises the strength of transition, see Ref. [49], and it is concluded that for sufficiently large suppression for EWBG the necessary condition is  $x \lesssim 0.03$ . However, the validity of this classical approximation is questionable, as thermal and quantum corrections can be expected to be important. However, for a reliable, non-perturbative determination of sphaleron rate, further studies are still required.

We emphasize that a systematic determination of most of the above quantities in the BSM theories that we consider, goes beyond the scope of research presented in this thesis, and are left for future work.

## Chapter 3

# Character and strength of EWPT in BSM theories

While the Standard Model with a single Higgs doublet has accurately met the phenomenological criteria set by collider experiments, the search for new physics continues. There is still room for a more complicated scalar sector, which continues to be an active subject of theoretical study. For concrete studies of the EWPT, we choose three different models, where the SM Higgs doublet is accompanied either by a new real scalar in the singlet or triplet representation of the  $SU(2)$  group, or by another Higgs doublet. Many other, typically more complicated, alternatives have been suggested and widely studied, including for example models, where the new singlet or triplet are complex rather than real, and models which combine any of these new types of scalars. For e.g. see Refs. [74–76] In this thesis, we shall for simplicity not discuss these more complicated models.

As the main topic of this thesis concerns the study of phase transition dynamics in the above BSM models, we choose not to discuss the viability of the models in light of collider data, i.e. how constrained their respective parameter spaces are. This is justified in the sense that our preliminary scans in any case only consider limited regions of the parameter spaces of the theories, while a more thorough scanning is still in progress. Once these more comprehensive scans are ready, it is crucial to extend our analysis to include up-to-date constraints from collider phenomenology before final conclusions about the properties of the EW phase transition in these models can be made.

In the present chapter we will apply results based on a nonperturbative analysis of the SM-like effective theory to the three aforementioned BSM theories. Before discussing the properties of the EWPT in different regions of the respective parameter spaces of these models, we present a compact introduction to each model as a brief physical motivation. For illustrative purposes, we begin by considering the phase transition in the pure SM case.

It should be recalled that in the articles presented in this thesis, the main emphasis was placed on the determination of the dimensional reduction matching relations between the full theories

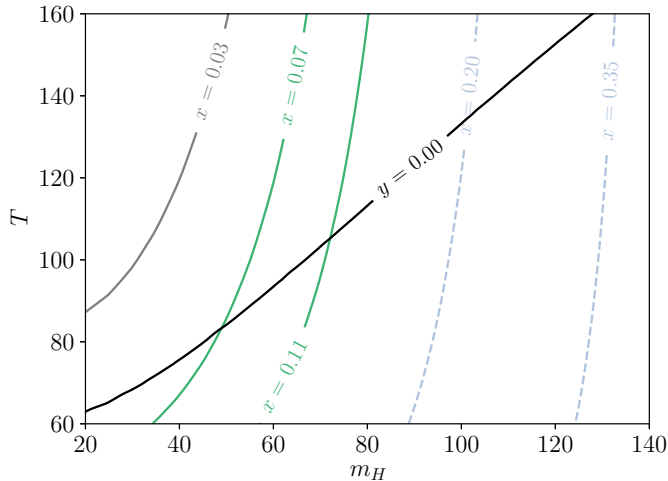


Figure 3.1: In the minimal SM, green solid contour lines in the vicinity of tree-level critical curve  $y = 0$  show region of first order transition ( $0 < x < 0.11$ ), while light gray dashed contours show crossover region ( $x > 0.11$ ). Gray solid contour  $x = 0.03$  never overlaps with  $y = 0$ .

and effective 3-d theories. To this end, quantitative predictions for many physical quantities and the properties of the EWPT were left for future study, which also limits the discussion of the present chapter. Apart from the case of the real-triplet extended SM, we shall also refrain from discussing the implications of our results to collider phenomenology, but leave this topic to more comprehensive future studies.

### 3.1 Standard Model

In the SM, the mass of the Higgs boson was a free parameter before its detection. In analogy to Fig. 8 of Ref. [70], in Fig. 3.1 we use the DR mapping in the minimal SM case to obtain the 3-d parameters  $x, y$  of Eq. (2.24) as functions of the Higgs mass  $m_H$  and the temperature  $T$ . The black line  $y = 0$  gives the tree-level value for the critical temperature  $T_c$ . The true, non-perturbatively determined  $T_c$  is known to lie very close to this line. For small Higgs masses, when  $0 < x < 0.11$ , the transition is of first order, and the critical end-point of the transition occurs when  $x \approx 0.11$ . For larger  $x$ , the transition is a cross-over. Importantly, the physical case with  $m_H = 125$  GeV corresponds to this last scenario, while smaller values of  $x$ , i.e. smaller  $m_H$ , would lead to stronger transitions. In Ref. [14], it was estimated that for viable EWBG it is required that  $x < 0.03$ . Therefore, the conclusion is that the EWBG would not have been viable in the SM for any  $m_H$ , as the  $x = 0.03$  curve never crosses the critical line  $y = 0$ , and the

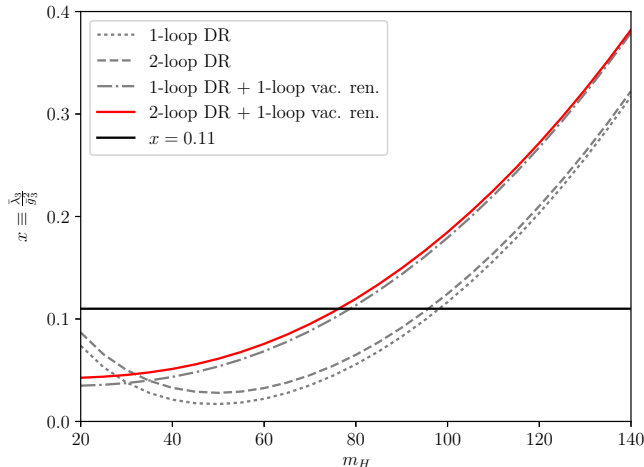


Figure 3.2: Critical value  $x_c = x(T_c)$  as function of the Higgs mass in the minimal SM, in different approximations for the dimensional reduction.

transition is always too weak to prevent the baryon washout in the broken phase.

In Fig. 3.2, the critical value  $x_c = x(T_c)$  is presented as a function of the Higgs mass, with different approximations applied in the process of dimensional reduction. The two-loop corrections to the 3-d mass parameters do not affect  $x$  directly, but only  $y$  and therefore  $T_c$ ; consequently, for  $x$  a two-loop evaluation is not crucial. However, carrying out a one-loop vacuum renormalisation that gives loop corrections to the  $\overline{\text{MS}}$ -parameters in terms of physical quantities, is clearly important for  $x$ , especially in the case of small Higgs masses.

In Fig. 3.3, the critical temperature of the transition is next shown as a function of the Higgs mass. In this case, two-loop improvement to the 3-d mass parameters has a bigger effect, as these corrections directly affect  $y$  parameter. In addition, one-loop vacuum renormalisation is again seen to be important.

For those BSM theories, and parameter regions thereof, that can be mapped into the same 3-d effective theory as the SM, an analysis of the character and strength of the phase transition can be performed in a similar manner, i.e. by finding the tree-level critical line  $y = 0$  and investigating the values of  $x$  along it. However, BSM theories typically contain more than one free parameter, making the analysis more complicated. In practice, we perform uniform scans of the full or restricted parameter space of a given model, finding the  $y = 0$  line by interpolation. Note that in order to identify the regions of first order transition, it is sufficient to use tree-level value for  $T_c$ , given by the line  $y = 0$ . However, if we wanted to obtain accurate values for the thermodynamic quantities discussed in the last section in specific points of the parameter space

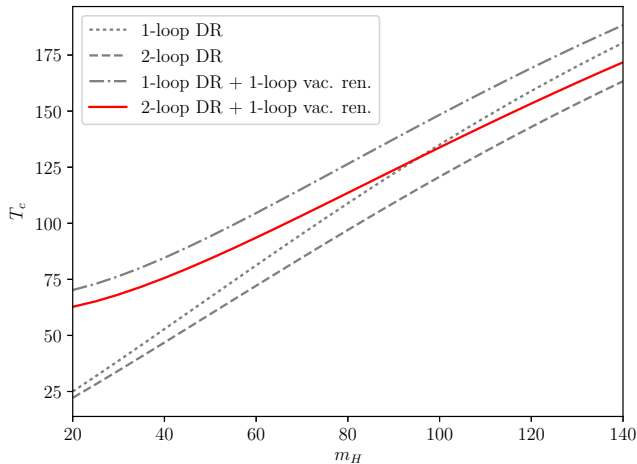


Figure 3.3: Similar to Fig 3.2, but with the critical temperature on the y-axis instead of  $x_c$ .

of a given model, one should use a next-to-leading order evaluation of  $T_c$ , utilizing information from the 3-d simulations.

Furthermore, in certain regions of the parameter space, mapping into the SM-like effective theory is not justified, as there is more than one light field present in the critical region that participate dynamically in the transition. In these regions, new simulations are required, leaving their quantitative analysis outside the scope of the present work.

## 3.2 Two-Higgs-Doublet Model

In the Two-Higgs-Doublet Model (2HDM), the SM is augmented with an additional scalar doublet, while the scalar potential reads

$$\begin{aligned}
 V(\phi_1, \phi_2) = & \mu_{11}^2 \phi_1^\dagger \phi_1 + \mu_{22}^2 \phi_2^\dagger \phi_2 + \mu_{12}^2 \phi_1^\dagger \phi_2 + \mu_{12}^{2*} \phi_2^\dagger \phi_1 \\
 & + \lambda_1 (\phi_1^\dagger \phi_1)^2 + \lambda_2 (\phi_2^\dagger \phi_2)^2 + \lambda_3 (\phi_1^\dagger \phi_1)(\phi_2^\dagger \phi_2) + \lambda_4 (\phi_1^\dagger \phi_2)(\phi_2^\dagger \phi_1) \\
 & + \frac{\lambda_5}{2} (\phi_1^\dagger \phi_2)^2 + \frac{\lambda_5^*}{2} (\phi_2^\dagger \phi_1)^2,
 \end{aligned} \tag{3.1}$$

with the index indicating the doublet in question. In writing down this potential, we have imposed a softly broken  $Z_2$ -symmetry, which means symmetry under  $\phi_i \rightarrow -\phi_i$  for either doublet, except for bilinear mixing terms that violate this symmetry. For a comprehensive review, see Ref. [77]. Only one of the doublets is assumed to couple to fermions, so that we avoid undesired flavor-changing neutral currents. In addition to the SM-like 125 GeV Higgs boson, the spectrum of the model includes two neutral – CP-even and -odd – Higgs bosons and two charged Higgs

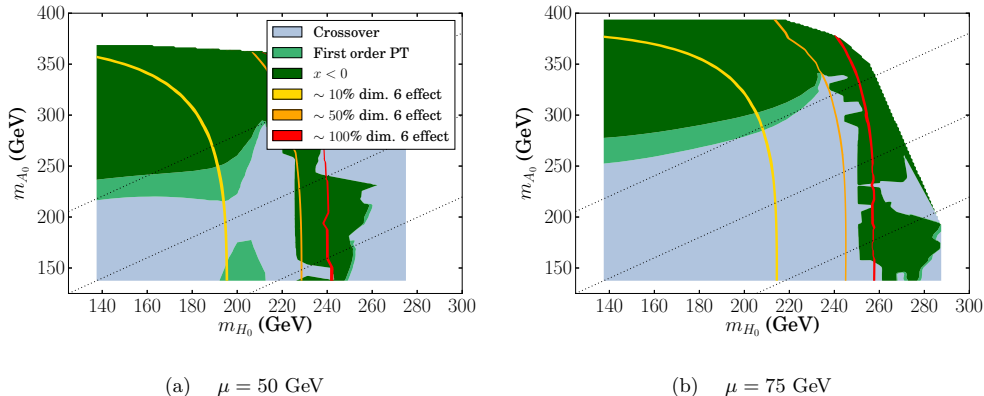


Figure 3.4: Slices of the 2HDM parameter space in the alignment limit where  $\tan(\beta) = 2$ . The coloured regions indicate the character of the EWPT and breakdown of dimensional reduction ( $x < 0$ ). The white regions are either rejected due to required physicality constraints or no transition is found in the temperature range 80-180 GeV.

bosons. The mixing and masses of these new scalars are constrained by collider experiments. In the 2HDM, a new source for CP violation is also provided, because complex couplings in the scalar potential lead to the mixing of neutral and imaginary parts of the doublets. Therefore, all ingredients required by EWBG are in principle realisable in this model. In terms of 4-d perturbation theory, previous studies include Refs. [37, 38, 78–83].

Rather surprisingly, in large parts of the 2HDM parameter space, the (thermo)dynamics of the 4-d theory near the transition point can be accurately described by an SM-like effective 3-d theory. When the non-zero Matsubara modes of the different fields are integrated out in the first step of DR, the resulting effective theory at heavy scale still contains two doublets in addition to heavy temporal scalar fields, of which the latter are integrated out in second step of DR. The remaining light theory contains only gauge fields and two scalar doublets with – generally – non-zero mixing. When this theory is diagonalized at the transition point, where one of the mass eigenvalues vanishes, the other turns out to be heavy. In other words, at the transition point it is justified to integrate out the other doublet in the second step of dimensional reduction, leaving behind an SM-like final effective 3-d theory. However, in some regions of the parameter space of the model, the EWPT may occur in two consecutive steps, where electroweak symmetry is broken to the direction of the new BSM degree of freedom at some temperature, but then restored in this direction at some lower temperature and finally broken to the SM – zero temperature – vacuum. In this scenario, there are more active light fields present during the transition than in the SM, and two dynamical doublets are required in accurate simulations. This means that new simulations need to be performed, implying that we will not consider this

scenario further in our work. For dimensional reduction in the 2HDM, see also Refs. [84, 85]

In the case of the SM-like effective theory, the thermodynamics of the system can be analyzed in terms of the old dimensionless 3-d parameters that are expressed in terms of the temperature and other physical quantities. The parameter space of the 2HDM with softly broken  $Z_2$ -symmetry is eight-dimensional. In paper II, we have restricted our study to the CP-conserving 2HDM, where  $\text{Im}(\lambda_5) = 0$  and  $\text{Im}(\mu_{12}^2) = 0$ .

In the case of the CP-conserving 2HDM, the free parameters correspond to the masses of the CP-even and -odd neutral Higgs bosons  $m_{H_0}$  and  $m_{A_0}$ , the mass charged Higgs boson mass  $m_{H^\pm}$ , the mixing angle  $\alpha$  between the CP-even scalars, the mixing of the vacuum expectation values, parametrized as  $\tan(\beta)$ , and finally the mixing mass parameter  $\mu^2 \equiv -\text{Re}(\mu_{12}^2)$ . Tree-level relations of these physical quantities and parameters that appear in the scalar potential of Eq. (3.1) can be found in Appendix B of Paper III.

A comprehensive scanning of the six-dimensional parameter space is still computationally expensive, but can be mitigated with a number of simplifications. Phenomenological studies of the model suggest that the charged Higgs mass should be degenerate with one of the neutral Higgs masses, so we may simplify the situation by setting  $m_{H^\pm} = m_{A_0}$ . In addition, we have decided to restrict our study to alignment limit, where  $\cos(\beta - \alpha) = 0$  and many collider constraints are automatically satisfied. The scanning of the remaining four-dimensional parameter space is straightforward, and in Fig. 3.4 we present two slices of the parameter space with the particular choice  $\tan(\beta) = 2.0$  and two different choices for  $\mu$ . In analogy to the SM case, we identify the character of the EWPT, i.e. regions of cross-over and first order transitions, from the value of the 3-d parameter  $x$ . The strength of the first-order transition is given by the magnitude of  $x$ : away from cross-over region,  $x$  decreases and the transition becomes stronger (with increasing latent heat and surface tension). In the white regions of the plots, parameter space points have either been rejected as non-physical (violating tree-level stability or unitarity constraints; see Appendix B of paper III), or there is no transition for any temperature in the scanned range (80-180 GeV).

However, unlike in the case of the SM, there are also regions where  $x$  is negative. In these regions, 3-d simulations are meaningless as the tree-level potential is not bounded from below. This signals the breakdown of dimensional reduction, which can be due to omitted higher order corrections to the parameters of the effective theory, or to neglected higher dimensional operators. Indeed, if we estimate the effect of the simplest dimension-6 operators  $(\phi_1^\dagger \phi_1)^3$  and  $(\phi_2^\dagger \phi_2)^3$  to the shift of the Higgs expectation value in the 3-d theory (see Section 3.2.3 in paper III), we observe in Fig. 3.4 that the resulting uncertainty in the results increases for decreasing  $x$ . We emphasize that performing a more comprehensive analysis of the effects of these dimension-6 operators is a huge task due to great number of different operators. Furthermore, 3-d simulations with higher-dimensional operators are not as straightforward due to the fact that super-renormalisability is lost, and lattice-continuum relations become more complicated.

At this early stage of our studies, it is not yet obvious how this breakdown of dimensional

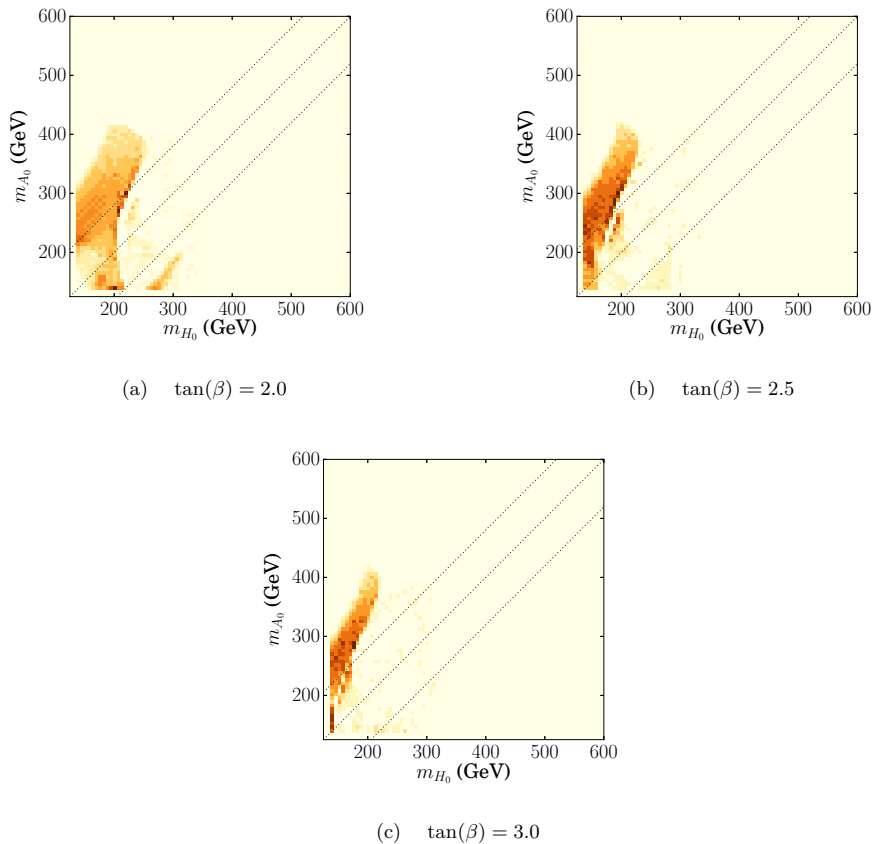


Figure 3.5: Heat maps with three different choices of  $\tan(\beta)$ , indicating the number of points with first order transition for different values of the mixing mass parameter  $\mu$ . For larger values of  $\tan(\beta)$ , region with the hierarchy  $m_{A_0} > m_{H_0} + m_Z$  clearly accomodates most of the points with first order transition.

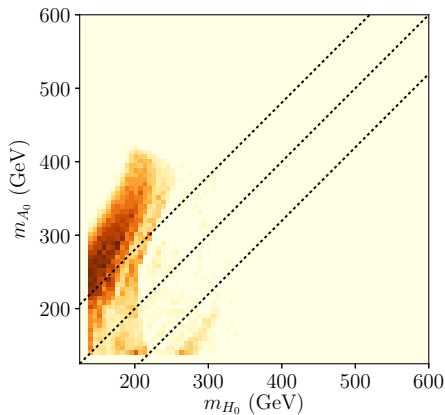


Figure 3.6: Combined heat map, showing number of points with first order transition for different mixing mass parameter  $\mu$  and  $\tan(\beta)$ . Figure by L. Niemi and D. J. Weir.

reduction should be handled and how trustworthy our current results concerning the character and strength of the transition are, as  $x$  turns rather rapidly from  $x = 0.11$  to negative. It nevertheless seems safe to conclude that in the regions where  $x$  is large (and dimensional reduction is certainly valid), the EWPT is of a cross-over type, in analogy with the SM. However, in order to draw interesting physical conclusions, we are eventually interested in regions of first-order transitions, where the effects of dimension-6 operators could be non-negligible.

Furthermore, we have performed uniform scans on the  $(m_{H_0}, m_{A_0})$ -plane with different fixed values of  $\tan(\beta)$  and  $\mu$  (for details of this scanning, see Section III in paper II). In Fig. 3.5, we highlight the regions of first order transition on the  $(m_{H_0}, m_{A_0})$ -plane by showing heat maps for varied values of  $\tan(\beta)$ , such that the color coding corresponds to the number of points for different choices of the mixing mass parameter  $\mu$  that produce a first order transition. In this manner, we lose some information about the  $\mu$ -dependence, but in exchange we can easily observe the overall trends. We observe that a first-order transition prefers the hierarchy condition  $m_{A_0} > m_{H_0} + m_Z$ , unless  $\tan(\beta) < 2$ . In Refs. [82, 83], a similar behavior was indeed found with a perturbative approach, and it was claimed that this hierarchy condition is the primary signature for a first order EWPT in the 2HDM.

In Fig. 3.6, we combine our data for different values of  $\tan(\beta)$  to produce an overall heat map (losing information on the specific dependence of both  $\mu$  and  $\tan(\beta)$ ). This plot shows some support for the claim about the aforementioned hierarchy condition being the primary signature of a first order transition in this model, yet it is clear that in other regions first order transitions are possible as well. However, the reliability of these preliminary results needs to be comprehensively investigated with more careful studies before conclusions can be made with

satisfactory accuracy. In particular, in our study in paper II physical quantities were related to  $\overline{\text{MS}}$ -parameters only at tree-level, while we expect one-loop corrections to be important.

### 3.3 Singlet extended Standard Model

In one of the simplest extensions of the SM, a real singlet scalar  $\sigma$  is included [86, 87], with the scalar potential

$$\begin{aligned}
 V(\phi, \sigma) = & -\mu_h^2 \phi^\dagger \phi + \lambda_h (\phi^\dagger \phi)^2 \\
 & + \frac{1}{2} \mu_\sigma^2 \sigma^2 + \mu_1 \sigma + \mu_3 \sigma^3 + \lambda_\sigma \sigma^4 \\
 & + \mu_m \sigma \phi^\dagger \phi + \lambda_m \sigma^2 \phi^\dagger \phi.
 \end{aligned}
 \tag{3.2}$$

where  $\phi$  denotes the ordinary SM Higgs doublet. The last line is frequently referred as a Higgs portal, as new field interacts only indirectly with the other SM fields, through their interactions with the Higgs. If a  $Z_2$ -symmetry – i.e. a symmetry under the transformation  $\phi \rightarrow -\phi$  or  $\sigma \rightarrow -\sigma$  – is imposed, the couplings  $\mu_1, \mu_3$  and  $\mu_m$  vanish, and  $\sigma$  becomes stable, making it a potential dark matter candidate.

In this model, there are no new sources of CP violation, so the EWBG cannot be viable without additional CP-violating operators, but the singlet can still affect the properties of the EWPT. If the  $Z_2$ -symmetry is not imposed, a mixing occurs between the singlet and doublet, of which the latter acquires a non-zero vacuum expectation value in the broken phase. The mass eigenstates are linear combinations of the singlet and doublet fields that both couple to the SM gauge fields and fermions. It is frequently assumed that the detected SM-like Higgs with a mass of 125 GeV corresponds to the mode with the lower mass eigenvalue. Compared to the pure SM, the mixing modifies the couplings of the Higgs boson to the other SM fields, as all couplings are suppressed by a cosine of the mixing angle. These modifications to the Higgs couplings are constrained, and couplings are required to be close to their SM limits.

In a perturbative determination of the effective potential, it is seen that at high temperatures the only minimum of the potential typically resides at the origin. For certain choices of the parameters of the model, a global minimum may also appear at  $\sigma \neq 0$ , but  $\phi = 0$ . When the temperature decreases, the potential develops a deeper minimum at  $\sigma = 0$  and  $\phi \neq 0$ , which breaks the electroweak symmetry. In this kind of a two-step transition, both the doublet and singlet will drive the transition, and the EWPT is qualitatively different than in the pure SM [88, 89]. For perturbative studies in this model, see Refs. [31, 32, 34].

In Paper I, dimensional reduction was carried out for the singlet extended SM in a limit where the new singlet was taken to be superheavy. This means that the singlet could be integrated out in the first step of dimensional reduction and does not appear in either of the 3-d theories. In this case, the parameters of the singlet can modify the one-step transition driven by the Higgs field, but the interesting two-step transition cannot be studied. Furthermore, in paper I regions

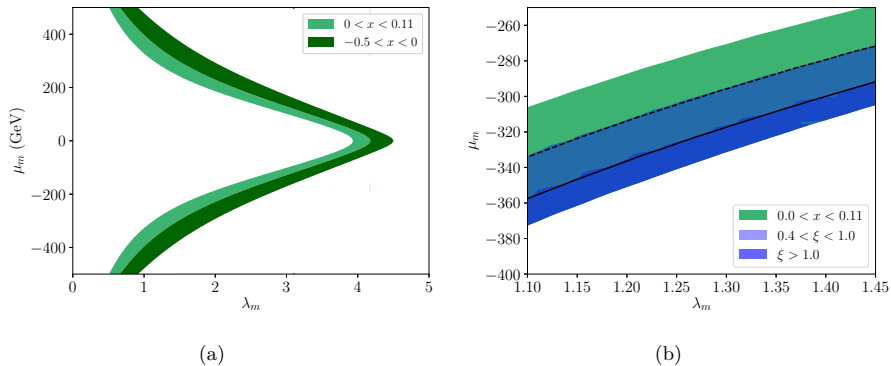


Figure 3.7: In (a) a slice of the singlet extended SM parameter space, with  $m_S = 400$  GeV,  $\mu_3 = 0$  GeV and  $\lambda_\sigma = 0.25$ . Again, the region  $0 < x < 0.11$  corresponds a first order transition, while the dimensional reduction procedure has broken down for  $x < 0$ . In (b), we take a closer look into a part of (a), supplemented by the result of perturbative analysis of 3-d theory in terms of  $\xi \equiv \phi_c^{4-d}/T_c$ . Countours of  $x = 0.07$  and  $x = 0.03$  are given by black dashed and solid curves, respectively.

of first order transition were not identified, but were left for future work. At the time of writing this thesis, this is still work in progress, but we present here preliminary results.

It turns out that 3-d parameters are not particularly sensitive to the quartic singlet self-interaction coupling  $\lambda_\sigma$ , and therefore we can fix the value of this parameter to any (perturbative) value. Furthermore, we simplify discussion by setting the cubic singlet self-interaction coupling  $\mu_3$  to zero. This leaves three parameters to be considered: the physical singlet mass  $m_S$  (related to the mass parameter  $\mu_\sigma^2$  at tree level) and two portal couplings  $\mu_m$  and  $\lambda_m$ . For different singlet masses, we find similar “boomerang” shaped regions in the  $(\lambda_m, \mu_m)$ -plane, as we illustrate in the case of  $m_S = 400$  GeV in Fig. 3.7a.

In Fig. 3.7b we finally demonstrate, how regions of first-order transitions can be found alternatively by applying perturbation theory in the 3-d theory. In this approach, we utilize the DR mapping of Paper I together with a 3-d effective potential derived in Ref. [68]. By finding  $T_c$  from the condition that the 3-d effective potential has two degenerate minima at the origin and at non-zero  $\phi_c^{3-d}$  (in Landau gauge), the strength of the transition can be characterized by  $\xi \equiv \phi_c^{4-d}/T_c$ . Note that by using the DR mapping, the 3-d field can be transformed into a 4-d one, see Eq. (3.60) in paper I. We observe that strong transitions with  $x < 0.03$  correspond to  $\xi > 1.0$ .

Further studies of the singlet extended Standard Model, addressing issues such as the importance of dimension-6 operators, phenomenological implications of our findings, as well as a comparison of the results to those obtained via 4-d perturbation theory, are still underway.

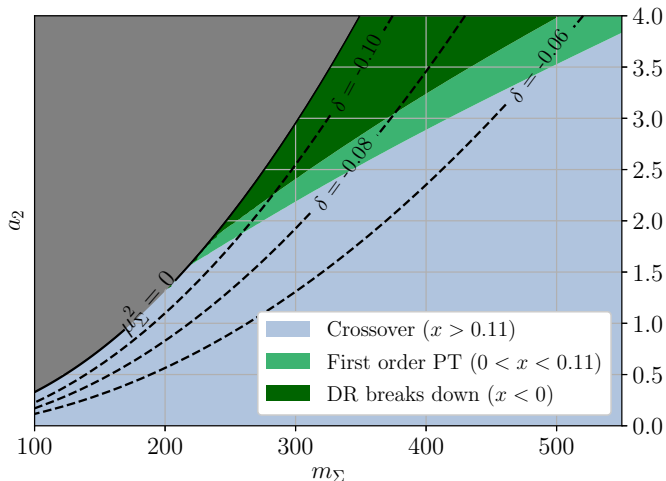


Figure 3.8: Character of a one-step transition, together with phenomenological constraint  $\delta$  – deviation to Higgs to digamma decay rate. We have fixed  $b_4 = 0.75$ . We have not scanned gray region where  $\mu_\sigma^2 > 0$ .

### 3.4 Standard Model with a real triplet

Another simple scalar extension of the SM is to accompany the theory by a real triplet  $\Sigma$  [39,90], with a Higgs portal type scalar potential of the form

$$\begin{aligned}
 V(\phi, \Sigma^a) = & -\mu_h^2 \phi^\dagger \phi + \lambda_h (\phi^\dagger \phi)^2 \\
 & -\frac{1}{2} \mu_\Sigma^2 \vec{\Sigma} \cdot \vec{\Sigma} + \frac{1}{2} b_4 (\vec{\Sigma} \cdot \vec{\Sigma})^2 \\
 & + a_2 \vec{\Sigma} \cdot \vec{\Sigma} \phi^\dagger \phi.
 \end{aligned} \tag{3.3}$$

We have imposed here a  $Z_2$  symmetry (i.e. symmetry under  $\phi \rightarrow -\phi$  or  $\vec{\Sigma} \rightarrow -\vec{\Sigma}$ ) for simplicity, as otherwise the allowed cubic term  $a_1 \phi^\dagger (\vec{\Sigma} \cdot \vec{\tau}) \phi$  (where  $\tau$  is a vector composed of Pauli matrices) would induce a vacuum expectation value for the neutral component of the triplet. This neutral triplet vev is tightly constrained by the electroweak  $\rho$ -parameter already at tree level, and consequently  $a_1$  would have to be very small. In addition to the neutral triplet, there are two new charged scalars, whose masses are nearly degenerate with the mass of the neutral component of the triplet. With  $Z_2$  symmetry, the neutral component of the triplet is stable and can serve as a cold dark matter candidate.

Because the triplet couples directly to the gauge field, the dynamics of this model can be tested in colliders by studying the decay of the Higgs boson into diphotons. This process is affected by the charged components of the triplet at one-loop level, which introduces deviations to the pure SM value. In this model, the EWPT can also occur via a two-step transition, see

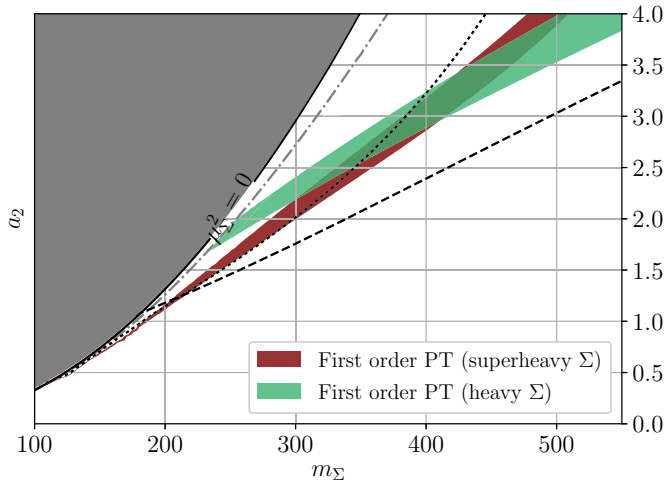


Figure 3.9: A comparison of heavy/superheavy approximations for the real triplet model. Black dashed and dotted curves denote the critical temperature  $T_c = 140$  GeV for heavy and superheavy cases, respectively, while gray dot/dashed curve indicates one-loop corrected  $\mu_\Sigma^2 = 0$  line.

Ref. [39]. However, as in the case of the real-singlet extension, there is no additional source of CP-violation in this model.

In the case of the real triplet extension of the SM, both the doublet and triplet fields can in general remain light near the phase transition, in which case the new scalar cannot be integrated out in the DR process without further assumptions. In particular, the transition can occur in two consecutive steps, so both scalars need to be dynamical in 3-d simulations. However, if one assumes that the mass of the triplet is so large that its  $\overline{\text{MS}}$  mass parameter is superheavy, i.e. of the order  $\pi T$ , then one can integrate the triplet out together with non-zero modes. In this case, the triplet never appears in the 3-d theory, but simply modifies the DR mapping between the full and effective theories. Alternatively, the mass of the triplet can be moderately heavy, so that one can integrate it out in second step of DR in the 3-d theory, along with the heavy temporal scalar fields. When the triplet is integrated out in the first or second step of dimensional reduction, what remains is a SM-like effective 3-d theory with a modified DR mapping.

In the real triplet extension of the SM, there are three free parameters: the neutral triplet mass  $M_\Sigma$ , the quartic portal coupling  $a_2$ , and the quartic triplet self-interaction coupling  $b_4$ . Note that the charged triplet mass is practically degenerate with the neutral triplet mass. It turns out – in analogy with the real singlet extension – that the 3-d parameters  $x, y$  are not very sensitive to the value of the self-interaction coupling  $b_4$ . In Fig. 3.8, we present the phase

structure of the model on the  $(M_\Sigma, a_2)$ -plane, focusing on the one-step transition region. In particular, we do not scan the region left of the black curve, where the triplet  $\overline{\text{MS}}$ -scheme mass parameter  $\mu_\Sigma^2 = 0$ , as in this region it would clearly not be justified to integrate the triplet out. In this region, we anticipate a two-step transition, as observed in the perturbative study of Ref. [39]. The dashed black curves indicate the value of  $\delta$  – a deviation of the Higgs to digamma decay rate compared to the SM value

$$\delta = \frac{\Gamma^{\Sigma\text{SM}}(h \rightarrow \gamma\gamma) - \Gamma^{\text{SM}}(h \rightarrow \gamma\gamma)}{\Gamma^{\text{SM}}(h \rightarrow \gamma\gamma)}. \quad (3.4)$$

In addition to displaying the first-order and cross-over regions, a key feature of Fig. 3.8 is the existence of a boundary between the two cases, which – we emphasize – cannot be obtained in a purely perturbative approach. At each point along this boundary, for a fixed  $M_\Sigma$ , there exists a minimum value for  $|\delta|$ . This would allow one to utilize a measurement of the Higgs to digamma decay rate to probe the character of the transition. However, a separate experimental study is required to measure  $M_\Sigma$ . If the mass of the neutral component were to be fixed by measurements, a sufficiently large negative  $\delta$  would imply a first order transition, while a smaller negative or a positive value would correspond to a cross-over.

Finally, in Fig. 3.9 we display a comparison between the heavy/superheavy approximations – whether the triplet is integrated out in the first or second step of dimensional reduction. The black dashed and dotted curves denote the critical temperature  $T_c = 140$  GeV for the heavy and superheavy cases, respectively. We observe that the locations of first order regions agree qualitatively, while the  $T_c$  curves show a larger discrepancy. We assume that this difference in the critical temperatures is related – at least partially – to our approximation in the superheavy case, where we have only used a one-loop level determination of the mass parameters that give  $y$  (see Appendix B in paper IV), from which  $T_c$  is subsequently solved.

# Chapter 4

## Review and outlook

The study of the electroweak phase transition in theories beyond the Standard Model is important in order to present accurate predictions for a possible stochastic gravitational wave background of cosmological origin. Furthermore, the problem of matter/antimatter asymmetry can be attempted to be solved with the electroweak baryogenesis, in which the generated baryon excess is sensitive to the properties of the transition. For both of these aspects, the new physics beyond the Standard Model is essential, and this provides a unique link between particle physics and cosmology.

In determining the properties of the electroweak phase transition in the Standard Model, non-perturbative methods have provided the most accurate results. Our aim is to generalise these non-perturbative studies to well-motivated BSM theories with extended Higgs sector. In the current literature, the standard method to analyse the properties of the transition is the perturbative evaluation of the finite-temperature effective potential in four dimensions. This approach is known to be inaccurate due to infrared properties of the thermal field theory in the vicinity of the phase transition. For this reason we have used a different approach based on dimensional reduction and construction of effective three dimensional theories. This makes it possible to perform efficient, non-perturbative Monte Carlo simulations that accurately capture the IR physics of the transition.

The main result of the research presented in this thesis are three-dimensional effective theories that were constructed for the Two-Higgs-Doublet Model and for the real singlet and real triplet extensions of the SM. These dimensional reduction mappings are a required ingredient for relating results of lattice simulations to the physical properties of the phase transition, and will form the basis of all our future studies on the subject.

In Paper I we performed the dimensional reduction for the Standard Model with a real singlet, in a limited region of the parameter space – where the singlet is integrated out – and with limited one-loop accuracy. Numerical analysis and generalisation of the dimensional reduction the case of the light singlet was left for future study. In Papers II and III we performed the dimensional reduction in the full parameter space of the model. Paper II was dedicated to presenting our results about character of the transition in the alignment limit of the CP-conserving 2HDM,

while details of the dimensional reduction were presented in Paper III. In this particular case of the 2HDM, our preliminary results showed some support for earlier perturbative studies, that claim that primary signature of the first order transition in this model is a mass degeneracy of the neutral Higgs bosons  $m_{A_0} > m_{H_0} + m_Z$ . However, further studies are required before final conclusions can be made. Finally, in Paper IV we performed the dimensional reduction in the full parameter space of the real triplet-extended Standard Model, and applied these results to part of parameter space where triplet can be integrated out. We found regions of strong first-order one-step transitions and considered phenomenological implications of this region for the Higgs to digamma decay rate. To achieve our goal of determining nonperturbatively the properties of the electroweak phase transition in several BSM theories with extended Higgs sectors, plenty of work still remains to be done.

At the time of writing, numerical results for the character of transition and comparison to perturbative analysis in the singlet-extended SM is in progress, as well as the generalisation of the dimensional reduction to the full parameter space of this model. In the future, we aim to perform new Monte Carlo simulations in this model where the singlet is dynamically included on lattice. Similar simulations are also planned for the triplet-extended Standard Model. These simulations are needed in order to study interesting two-step transitions in these models. In the 2HDM, more general parameter space scans are currently underway. In all three of these models, determination of the equilibrium thermodynamic quantities, such as critical temperature (beyond leading order), latent heat and surface tension is still a work in progress. Nonperturbative computations of the non-equilibrium properties, such as bubble nucleation and sphaleron transition rates, are left for future work.

Furthermore, in addition to performing new simulations and extracting the interesting physical quantities of the transition, the accuracy of the dimensional reduction has to be addressed more carefully. Indeed, we aim to perform a comprehensive comparison of different methods to analyse the phase transition in these scalar extensions of the SM. This comparison would include determination of the same quantities by three-dimensional approach, by four-dimensional perturbation theory and furthermore by four-dimensional lattice simulations without fermions. This kind of systematic comparison would allow us to reduce theoretical uncertainties and, furthermore, set a definite benchmarks for the accuracy that can be obtained by the frequently used perturbative approach, in contrast to non-perturbative methods.

Finally, in the future it would be extremely valuable to automatise the dimensional reduction calculation into a package that outputs the coefficients of the 3-d theories for a given input 4-d theory, together with a perturbative finite-temperature effective potential. By using the background field method to calculate static correlators and the effective potential, at least at one-loop accuracy this goal could be realistically achieved in near future. Automatisation of these calculations would be particularly important in theories with more complicated scalar sector.

It is possible that in the future LISA detects a gravitational wave signal from the early

universe. In the long run, our research takes important steps towards providing a theoretical understanding of such signatures and their relation to underlying models of elementary particle physics. At the same time, same same results can be used to advance our understanding of the matter/antimatter asymmetry of the universe.



# Bibliography

- [1] Tomáš Brauner, Tuomas V. I. Tenkanen, Anders Tranberg, Alekski Vuorinen, and David J. Weir. Dimensional reduction of the Standard Model coupled to a new singlet scalar field. *JHEP*, 03:007, 2017, 1609.06230.
- [2] Jens O. Andersen, Tyler Gorda, Andreas Helset, Lauri Niemi, Tuomas V. I. Tenkanen, Anders Tranberg, Alekski Vuorinen, and David J. Weir. On the nature of the electroweak phase transition in the two Higgs doublet model. 2017, 1711.09849.
- [3] Tyler Gorda, Andreas Helset, Lauri Niemi, Tuomas V. I. Tenkanen, and David J. Weir. Electroweak phase transition and dimensional reduction of the Two-Higgs-Doublet Model. 2018, 1802.05056.
- [4] Lauri Niemi, Hiren H. Patel, Michael J. Ramsey-Musolf, Tuomas V. I. Tenkanen, and David J. Weir. Electroweak phase transition in the  $\Sigma$ SM - I: Dimensional reduction. 2018, 1802.10500.
- [5] Georges Aad et al. Observation of a new particle in the search for the Standard Model Higgs boson with the ATLAS detector at the LHC. *Phys. Lett.*, B716:1–29, 2012, 1207.7214.
- [6] Serguei Chatrchyan et al. Observation of a new boson at a mass of 125 GeV with the CMS experiment at the LHC. *Phys. Lett.*, B716:30–61, 2012, 1207.7235.
- [7] B. P. Abbott et al. Observation of Gravitational Waves from a Binary Black Hole Merger. *Phys. Rev. Lett.*, 116(6):061102, 2016, 1602.03837.
- [8] B. P. Abbott et al. GW170817: Observation of Gravitational Waves from a Binary Neutron Star Inspiral. *Phys. Rev. Lett.*, 119(16):161101, 2017, 1710.05832.
- [9] P. Amaro-Seoane, H. Audley, S. Babak, J. Baker, E. Barausse, P. Bender, E. Berti, P. Binetruy, M. Born, D. Bortoluzzi, J. Camp, C. Caprini, V. Cardoso, M. Colpi, J. Conklin, N. Cornish, C. Cutler, K. Danzmann, R. Dolesi, L. Ferraioli, V. Ferroni, E. Fitzsimons, J. Gair, L. Gesa Bote, D. Giardini, F. Gibert, C. Grimani, H. Halloin, G. Heinzl, T. Hertog, M. Hewitson, K. Holley-Bockelmann, D. Hollington, M. Hueller, H. Inchauspe, P. Jetzer, N. Karnesis, C. Killow, A. Klein, B. Klipstein, N. Korsakova, S. L Larson, J. Livas, I. Lloro, N. Man, D. Mance, J. Martino, I. Mateos, K. McKenzie, S. T McWilliams, C. Miller, G. Mueller, G. Nardini, G. Nelemans, M. Nofrarias, A. Petiteau, P. Pivato, E. Plagnol, E. Porter, J. Reiche, D. Robertson, N. Robertson, E. Rossi, G. Russano,

- B. Schutz, A. Sesana, D. Shoemaker, J. Slutsky, C. F. Sopuerta, T. Sumner, N. Tamanini, I. Thorpe, M. Troebs, M. Vallisneri, A. Vecchio, D. Vetrugno, S. Vitale, M. Volonteri, G. Wanner, H. Ward, P. Wass, W. Weber, J. Ziemer, and P. Zweifel. Laser Interferometer Space Antenna. *ArXiv e-prints*, February 2017, 1702.00786.
- [10] Chiara Caprini et al. Science with the space-based interferometer eLISA. II: Gravitational waves from cosmological phase transitions. *JCAP*, 1604(04):001, 2016, 1512.06239.
- [11] Chiara Caprini and Daniel G. Figueroa. Cosmological Backgrounds of Gravitational Waves. 2018, 1801.04268.
- [12] Steven Weinberg. Gauge and Global Symmetries at High Temperature. *Phys. Rev.*, D9:3357–3378, 1974.
- [13] D. A. Kirzhnits and Andrei D. Linde. Symmetry Behavior in Gauge Theories. *Annals Phys.*, 101:195–238, 1976.
- [14] K. Kajantie, M. Laine, K. Rummukainen, and Mikhail E. Shaposhnikov. The Electroweak phase transition: A Nonperturbative analysis. *Nucl. Phys.*, B466:189–258, 1996, hep-lat/9510020.
- [15] K. Kajantie, M. Laine, K. Rummukainen, and Mikhail E. Shaposhnikov. Is there a hot electroweak phase transition at  $m(H)$  larger or equal to  $m(W)$ ? *Phys. Rev. Lett.*, 77:2887–2890, 1996, hep-ph/9605288.
- [16] K. Kajantie, M. Laine, K. Rummukainen, and Mikhail E. Shaposhnikov. A Nonperturbative analysis of the finite T phase transition in  $SU(2) \times U(1)$  electroweak theory. *Nucl. Phys.*, B493:413–438, 1997, hep-lat/9612006.
- [17] F. Csikor, Z. Fodor, and J. Heitger. Endpoint of the hot electroweak phase transition. *Phys. Rev. Lett.*, 82:21–24, 1999, hep-ph/9809291.
- [18] Laurent Canetti, Marco Drewes, and Mikhail Shaposhnikov. Matter and Antimatter in the Universe. *New J. Phys.*, 14:095012, 2012, 1204.4186.
- [19] V. A. Kuzmin, V. A. Rubakov, and M. E. Shaposhnikov. On the Anomalous Electroweak Baryon Number Nonconservation in the Early Universe. *Phys. Lett.*, 155B:36, 1985.
- [20] David J. Weir. Gravitational waves from a first order electroweak phase transition: a brief review. *Phil. Trans. Roy. Soc. Lond.*, A376:20170126, 2018, 1705.01783.
- [21] James M. Cline. Baryogenesis. In *Les Houches Summer School - Session 86: Particle Physics and Cosmology: The Fabric of Spacetime Les Houches, France, July 31-August 25, 2006*, 2006, hep-ph/0609145.
- [22] David E. Morrissey and Michael J. Ramsey-Musolf. Electroweak baryogenesis. *New J. Phys.*, 14:125003, 2012, 1206.2942.
- [23] Graham Albert White. *A Pedagogical Introduction to Electroweak Baryogenesis*. IOP Concise Physics. Morgan & Claypool, 2016.

- [24] Mikko Laine and Aleksi Vuorinen. Basics of Thermal Field Theory. *Lect. Notes Phys.*, 925:pp.1–281, 2016, 1701.01554.
- [25] Sidney Coleman. Fate of the false vacuum: Semiclassical theory. *Phys. Rev. D*, 15:2929–2936, May 1977.
- [26] Paul Joseph Steinhardt. Relativistic detonation waves and bubble growth in false vacuum decay. *Phys. Rev. D*, 25:2074–2085, Apr 1982.
- [27] Edward Witten. Cosmic separation of phases. *Phys. Rev. D*, 30:272–285, Jul 1984.
- [28] C. J. Hogan. Gravitational radiation from cosmological phase transitions. *Mon. Not. Roy. Astron. Soc.*, 218:629–636, 1986.
- [29] Mark Hindmarsh, Stephan J. Huber, Kari Rummukainen, and David J. Weir. Gravitational waves from the sound of a first order phase transition. *Phys. Rev. Lett.*, 112:041301, 2014, 1304.2433.
- [30] Michela D’Onofrio and Kari Rummukainen. Standard model cross-over on the lattice. *Phys. Rev. D*, 93:025003, Jan 2016.
- [31] Vernon Barger, Paul Langacker, Mathew McCaskey, Michael J. Ramsey-Musolf, and Gabe Shaughnessy. Cern lhc phenomenology of an extended standard model with a real scalar singlet. *Phys. Rev. D*, 77:035005, Feb 2008.
- [32] Stefano Profumo, Michael J. Ramsey-Musolf, and Gabe Shaughnessy. Singlet higgs phenomenology and the electroweak phase transition. *Journal of High Energy Physics*, 2007(08):010, 2007.
- [33] Ville Vaskonen. Electroweak baryogenesis and gravitational waves from a real scalar singlet. *Phys. Rev. D*, 95:123515, Jun 2017.
- [34] Ankit Beniwal, Marek Lewicki, James D. Wells, Martin White, and Anthony G. Williams. Gravitational wave, collider and dark matter signals from a scalar singlet electroweak baryogenesis. *Journal of High Energy Physics*, 2017(8):108, Aug 2017.
- [35] Chien-Yi Chen, Jonathan Kozaczuk, and Ian M. Lewis. Non-resonant collider signatures of a singlet-driven electroweak phase transition. *Journal of High Energy Physics*, 2017(8):96, Aug 2017.
- [36] James M. Cline and Pierre-Anthony Lemieux. Electroweak phase transition in two higgs doublet models. *Phys. Rev. D*, 55:3873–3881, Mar 1997.
- [37] Lars Fromme, Stephan J. Huber, and Michael Seniuch. Baryogenesis in the two-higgs doublet model. *Journal of High Energy Physics*, 2006(11):038, 2006.
- [38] G. C. Dorsch, S. J. Huber, and J. M. No. A strong electroweak phase transition in the 2HDM after LHC8. *JHEP*, 10:029, 2013, 1305.6610.
- [39] Hiren H. Patel and Michael J. Ramsey-Musolf. Stepping Into Electroweak Symmetry Breaking: Phase Transitions and Higgs Phenomenology. *Phys. Rev.*, D88:035013, 2013, 1212.5652.

- [40] Andrei D. Linde. Infrared Problem in Thermodynamics of the Yang-Mills Gas. *Phys. Lett.*, 96B:289–292, 1980.
- [41] David J. Gross, Robert D. Pisarski, and Laurence G. Yaffe. QCD and Instantons at Finite Temperature. *Rev. Mod. Phys.*, 53:43, 1981.
- [42] Hiren H. Patel and Michael J. Ramsey-Musolf. Baryon Washout, Electroweak Phase Transition, and Perturbation Theory. *JHEP*, 07:029, 2011, 1101.4665.
- [43] M. Laine. The Two loop effective potential of the 3-d SU(2) Higgs model in a general covariant gauge. *Phys. Lett.*, B335:173–178, 1994, hep-ph/9406268.
- [44] K. Farakos, K. Kajantie, K. Rummukainen, and Mikhail E. Shaposhnikov. 3-d physics and the electroweak phase transition: A Framework for lattice Monte Carlo analysis. *Nucl. Phys.*, B442:317–363, 1995, hep-lat/9412091.
- [45] Mark Hindmarsh, Stephan J. Huber, Kari Rummukainen, and David J. Weir. Shape of the acoustic gravitational wave power spectrum from a first order phase transition. *Phys. Rev.*, D96(10):103520, 2017, 1704.05871.
- [46] Pedro Schwaller. Gravitational Waves from a Dark Phase Transition. *Phys. Rev. Lett.*, 115(18):181101, 2015, 1504.07263.
- [47] S. Eidelman et al. Review of particle physics. Particle Data Group. *Phys. Lett.*, B592(1-4):1–5, 2004.
- [48] P. A. R. Ade et al. Planck 2013 results. XVI. Cosmological parameters. *Astron. Astrophys.*, 571:A16, 2014, 1303.5076.
- [49] V. A. Rubakov and M. E. Shaposhnikov. Electroweak baryon number nonconservation in the early universe and in high-energy collisions. *Usp. Fiz. Nauk*, 166:493–537, 1996, hep-ph/9603208. [*Phys. Usp.*39,461(1996)].
- [50] M. Fukugita and T. Yanagida. Baryogenesis Without Grand Unification. *Phys. Lett.*, B174:45–47, 1986.
- [51] Ian Affleck and Michael Dine. A New Mechanism for Baryogenesis. *Nucl. Phys.*, B249:361–380, 1985.
- [52] Stephon Haigh-Solom Alexander, Michael E. Peskin, and Mohammad M. Sheikh-Jabbari. Leptogenesis from gravity waves in models of inflation. *Phys. Rev. Lett.*, 96:081301, 2006, hep-th/0403069.
- [53] Alexander Kusenko, Lauren Pearce, and Louis Yang. Postinflationary Higgs relaxation and the origin of matter-antimatter asymmetry. *Phys. Rev. Lett.*, 114(6):061302, 2015, 1410.0722.
- [54] A. D. Sakharov. Violation of CP Invariance, c Asymmetry, and Baryon Asymmetry of the Universe. *Pisma Zh. Eksp. Teor. Fiz.*, 5:32–35, 1967. [*Usp. Fiz. Nauk*161,61(1991)].
- [55] Stephen L. Adler. Axial vector vertex in spinor electrodynamics. *Phys. Rev.*, 177:2426–2438, 1969.

- [56] J. S. Bell and R. Jackiw. A PCAC puzzle:  $\pi^0 \rightarrow \gamma \gamma$  in the sigma model. *Nuovo Cim.*, A60:47–61, 1969.
- [57] N. S. Manton. Topology in the Weinberg-Salam Theory. *Phys. Rev.*, D28:2019, 1983.
- [58] Frans R. Klinkhamer and N. S. Manton. A Saddle Point Solution in the Weinberg-Salam Theory. *Phys. Rev.*, D30:2212, 1984.
- [59] Peter Brockway Arnold and Larry D. McLerran. Sphalerons, Small Fluctuations and Baryon Number Violation in Electroweak Theory. *Phys. Rev.*, D36:581, 1987.
- [60] Peter Brockway Arnold and Larry D. McLerran. The Sphaleron Strikes Back. *Phys. Rev.*, D37:1020, 1988.
- [61] Glennys R. Farrar and M. E. Shaposhnikov. Baryon asymmetry of the universe in the minimal Standard Model. *Phys. Rev. Lett.*, 70:2833–2836, 1993, hep-ph/9305274. [Erratum: *Phys. Rev. Lett.* 71,210(1993)].
- [62] Glennys R. Farrar and M. E. Shaposhnikov. Baryon asymmetry of the universe in the standard electroweak theory. *Phys. Rev.*, D50:774, 1994, hep-ph/9305275.
- [63] M. B. Gavela, P. Hernandez, J. Orloff, O. Pene, and C. Quimbay. Standard model CP violation and baryon asymmetry. Part 2: Finite temperature. *Nucl. Phys.*, B430:382–426, 1994, hep-ph/9406289.
- [64] Tomas Brauner, Olli Taanila, Anders Tranberg, and Aleksi Vuorinen. Temperature Dependence of Standard Model CP Violation. *Phys. Rev. Lett.*, 108:041601, 2012, 1110.6818.
- [65] Tomas Brauner, Olli Taanila, Anders Tranberg, and Aleksi Vuorinen. Computing the temperature dependence of effective CP violation in the standard model. *JHEP*, 11:076, 2012, 1208.5609.
- [66] José M. No. Large gravitational wave background signals in electroweak baryogenesis scenarios. *Phys. Rev. D*, 84:124025, Dec 2011.
- [67] Mariano Quiros. Finite temperature field theory and phase transitions. In *Proceedings, Summer School in High-energy physics and cosmology: Trieste, Italy, June 29-July 17, 1998*, pages 187–259, 1999, hep-ph/9901312.
- [68] K. Farakos, K. Kajantie, K. Rummukainen, and Mikhail E. Shaposhnikov. 3-D physics and the electroweak phase transition: Perturbation theory. *Nucl. Phys.*, B425:67–109, 1994, hep-ph/9404201.
- [69] Thomas Appelquist and J. Carazzone. Infrared singularities and massive fields. *Phys. Rev. D*, 11:2856–2861, May 1975.
- [70] K. Kajantie, M. Laine, K. Rummukainen, and Mikhail E. Shaposhnikov. Generic rules for high temperature dimensional reduction and their application to the standard model. *Nucl. Phys.*, B458:90–136, 1996, hep-ph/9508379.
- [71] Eric Braaten and Agustin Nieto. Effective field theory approach to high temperature thermodynamics. *Phys. Rev.*, D51:6990–7006, 1995, hep-ph/9501375.

- [72] James M. Cline and Kimmo Kainulainen. Supersymmetric electroweak phase transition: Beyond perturbation theory. *Nucl. Phys.*, B482:73–91, 1996, hep-ph/9605235.
- [73] James M. Cline and Kimmo Kainulainen. Supersymmetric electroweak phase transition: Dimensional reduction versus effective potential. *Nucl. Phys.*, B510:88–102, 1998, hep-ph/9705201.
- [74] Margarete Mühlleitner, Marco O. P. Sampaio, Rui Santos, and Jonas Wittbrodt. Phenomenological Comparison of Models with Extended Higgs Sectors. *JHEP*, 08:132, 2017, 1703.07750.
- [75] Tommi Alanne, Kimmo Kainulainen, Kimmo Tuominen, and Ville Vaskonen. Baryogenesis in the two doublet and inert singlet extension of the Standard Model. *JCAP*, 1608(08):057, 2016, 1607.03303.
- [76] Shehu S. AbdusSalam and Talal Ahmed Chowdhury. Scalar Representations in the Light of Electroweak Phase Transition and Cold Dark Matter Phenomenology. *JCAP*, 1405:026, 2014, 1310.8152.
- [77] G. C. Branco, P. M. Ferreira, L. Lavoura, M. N. Rebelo, Marc Sher, and Joao P. Silva. Theory and phenomenology of two-Higgs-doublet models. *Phys. Rept.*, 516:1–102, 2012, 1106.0034.
- [78] James M. Cline, Kimmo Kainulainen, and Axel P. Vischer. Dynamics of two Higgs doublet CP violation and baryogenesis at the electroweak phase transition. *Phys. Rev.*, D54:2451–2472, 1996, hep-ph/9506284.
- [79] P. Basler, M. Krause, M. Muhlleitner, J. Wittbrodt, and A. Wlotzka. Strong First Order Electroweak Phase Transition in the CP-Conserving 2HDM Revisited. *JHEP*, 02:121, 2017, 1612.04086.
- [80] Philipp Basler, Margarete Mühlleitner, and Jonas Wittbrodt. The CP-Violating 2HDM in Light of a Strong First Order Electroweak Phase Transition and Implications for Higgs Pair Production. 2017, 1711.04097.
- [81] G. C. Dorsch, S. J. Huber, T. Konstandin, and J. M. No. A Second Higgs Doublet in the Early Universe: Baryogenesis and Gravitational Waves. *JCAP*, 1705(05):052, 2017, 1611.05874.
- [82] G. C. Dorsch, S. J. Huber, K. Mimasu, and J. M. No. Echoes of the Electroweak Phase Transition: Discovering a second Higgs doublet through  $A_0 \rightarrow ZH_0$ . *Phys. Rev. Lett.*, 113(21):211802, 2014, 1405.5537.
- [83] G. C. Dorsch, S. J. Huber, K. Mimasu, and J. M. No. The Higgs Vacuum Uplifted: Revisiting the Electroweak Phase Transition with a Second Higgs Doublet. *JHEP*, 12:086, 2017, 1705.09186.
- [84] Marta Losada. High temperature dimensional reduction of the MSSM and other multiscalar models. *Phys. Rev.*, D56:2893–2913, 1997, hep-ph/9605266.

- 
- [85] Jens O. Andersen. Dimensional reduction of the two Higgs doublet model at high temperature. *Eur. Phys. J.*, C11:563–570, 1999, hep-ph/9804280.
- [86] Vernon Barger, Paul Langacker, Mathew McCaskey, Michael J. Ramsey-Musolf, and Gabe Shaughnessy. LHC Phenomenology of an Extended Standard Model with a Real Scalar Singlet. *Phys. Rev.*, D77:035005, 2008, 0706.4311.
- [87] A. Ashoorioon and T. Konstandin. Strong electroweak phase transitions without collider traces. *JHEP*, 07:086, 2009, 0904.0353.
- [88] Satoru Inoue, Grigory Ovanessian, and Michael J. Ramsey-Musolf. Two-Step Electroweak Baryogenesis. *Phys. Rev.*, D93:015013, 2016, 1508.05404.
- [89] Nikita Blinov, Jonathan Kozaczuk, David E. Morrissey, and Carlos Tamarit. Electroweak Baryogenesis from Exotic Electroweak Symmetry Breaking. *Phys. Rev.*, D92(3):035012, 2015, 1504.05195.
- [90] Pavel Fileviez Perez, Hiren H. Patel, Michael J. Ramsey-Musolf, and Kai Wang. Triplet Scalars and Dark Matter at the LHC. *Phys. Rev.*, D79:055024, 2009, 0811.3957.